Modern Methods in Heterogeneous Catalysis

Class 2007/2008

Vibrational Spectroscopy

Spectroscopy in catalysis

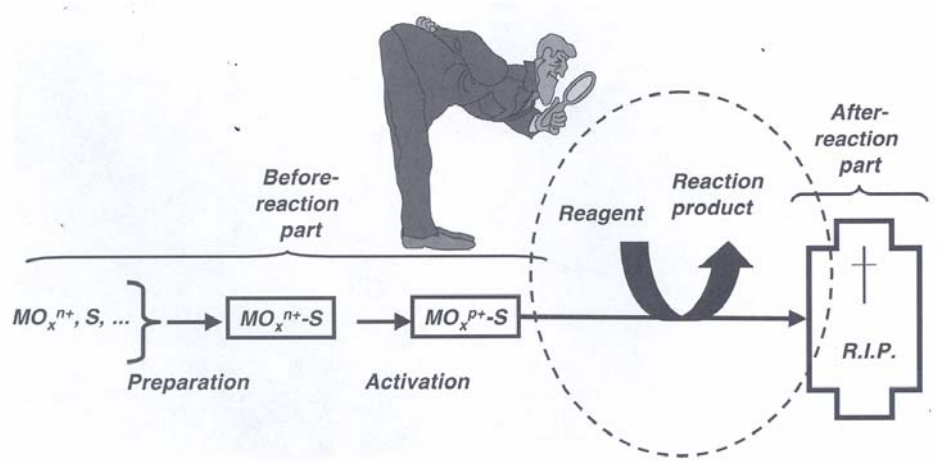

Figure 6. The lifespan of a catalyst, indicating the preparation, activation, catalytic event and deactivation process of the catalyst material. M, O and S are the transition metal ion, oxygen and support, respectively. The superscripts refer to the oxidation state of the metal ion.

Models in heterogeneous catalysis research

powder catalyst

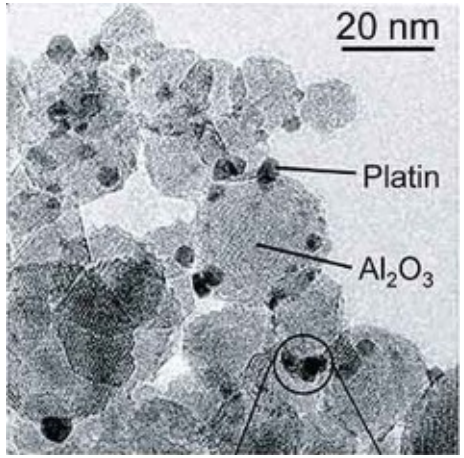

metal clusters on single crystals

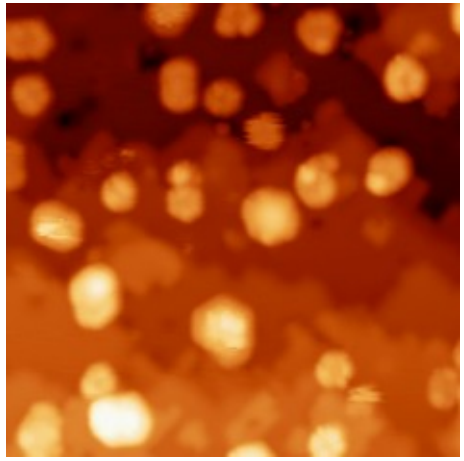

metal single crystals

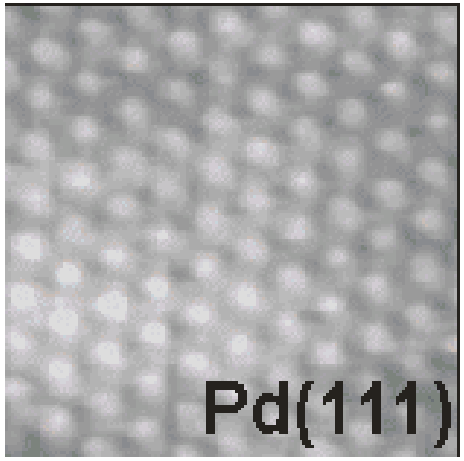

Table 2. Research strategies available to relate the physicochemical properties of catalysts with their catalytic performances. The *in-situ* characterization techniques covered in this book are indicated in italics.

Measurement conditions	Real catalyst material	Single crystal model catalyst
Reaction conditions	*Infrared spectroscopy*	Infrared spectroscopy
	Raman spectroscopy	Sum-frequency generation-surface specific vibrational spectroscopy
	Extended X-ray absorption fine structure	Scanning tunneling microscopy
	X-ray absorption near edge spectroscopy	Atomic force microscopy
	Nuclear magnetic resonance	Temperature programmed techniques
	Electron paramagnetic resonance	
	Ultraviolet-visible spectroscopy	
	X-ray diffraction	
	Small angle and wide angle X-ray scattering	
	Positron emission tomography and profiling	
	Atomic force microscopy	
	Mössbauer spectroscopy	
	Temperature programmed techniques, such as temperature programmed desorption and temperature programmed oxidation	
Vacuum conditions (in some cases measurements in millibar conditions in the presence of a reactant are already possible)	X-ray photoelectron spectroscopy	All surface science techniques
	Ultraviolet photoelectron spectroscopy	
	Auger electron spectroscopy	
	Secondary ion mass spectrometry	
	Secondary neutral mass spectrometry	
	Low energy ion scattering	
	Rutherford backscattering	
	Transmission electron microscopy	
	Scanning electron microscopy	

Vibrational spectroscopy

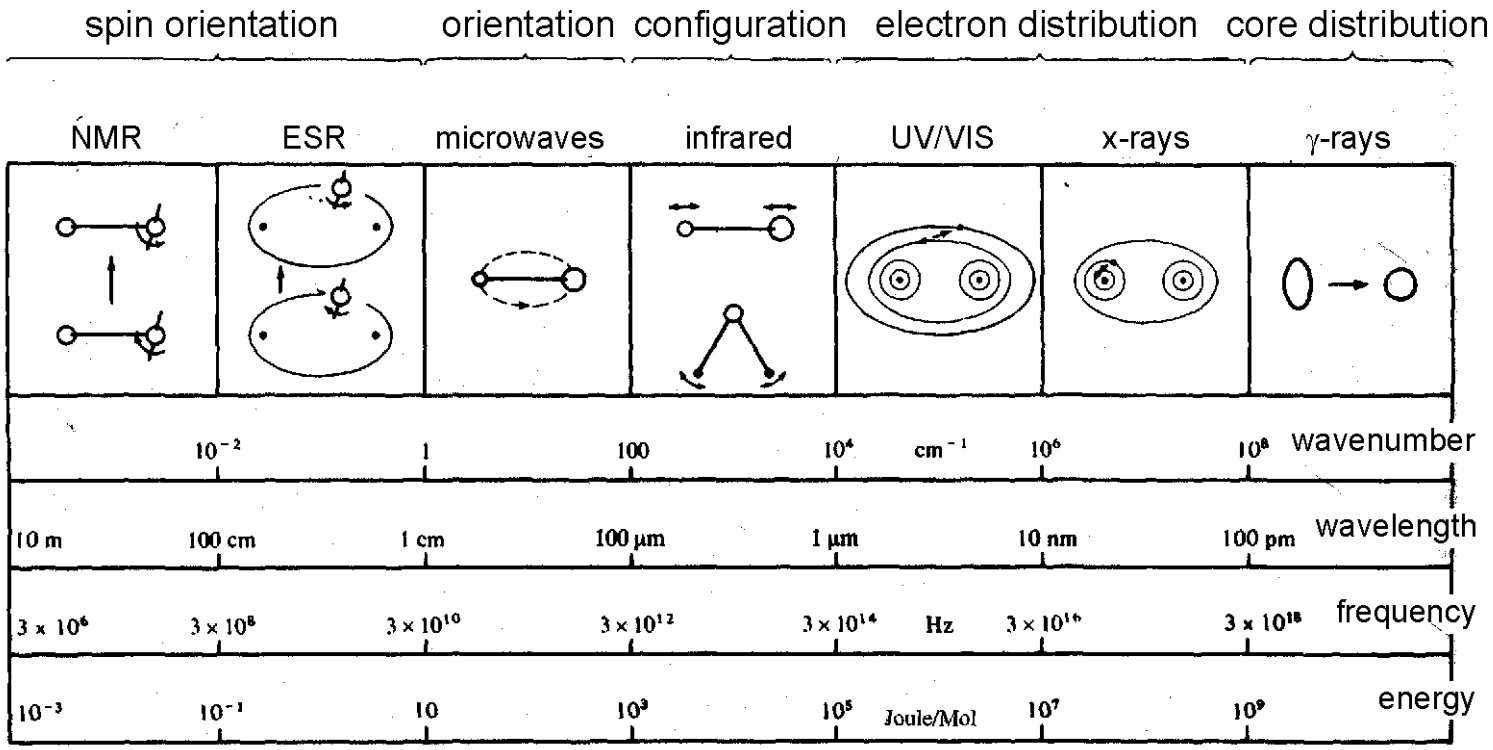

1 eV = 96.485 kJ/mol = 8065.5 cm^{-1}

Table 8.1: Classification of infrared radiation.

Region	Wavelength (µm)	Energy (meV) [a]	Frequency (cm^{-1})	Detection of
Infrared	1000–1	1.2–1240	10–10000	
Far	1000–50	1.2–25	10–200	Lattice Vibrations
Mid	50–2.5	25–496	200–4000	Molecular Vibrations
Near	2.5–1	496–1240	4000–10000	Overtones

a) 1 meV = 8.0655 cm^{-1}

Group frequency concept

Functional groups can be treated independently from the rest of the molecule.
Chemical identification

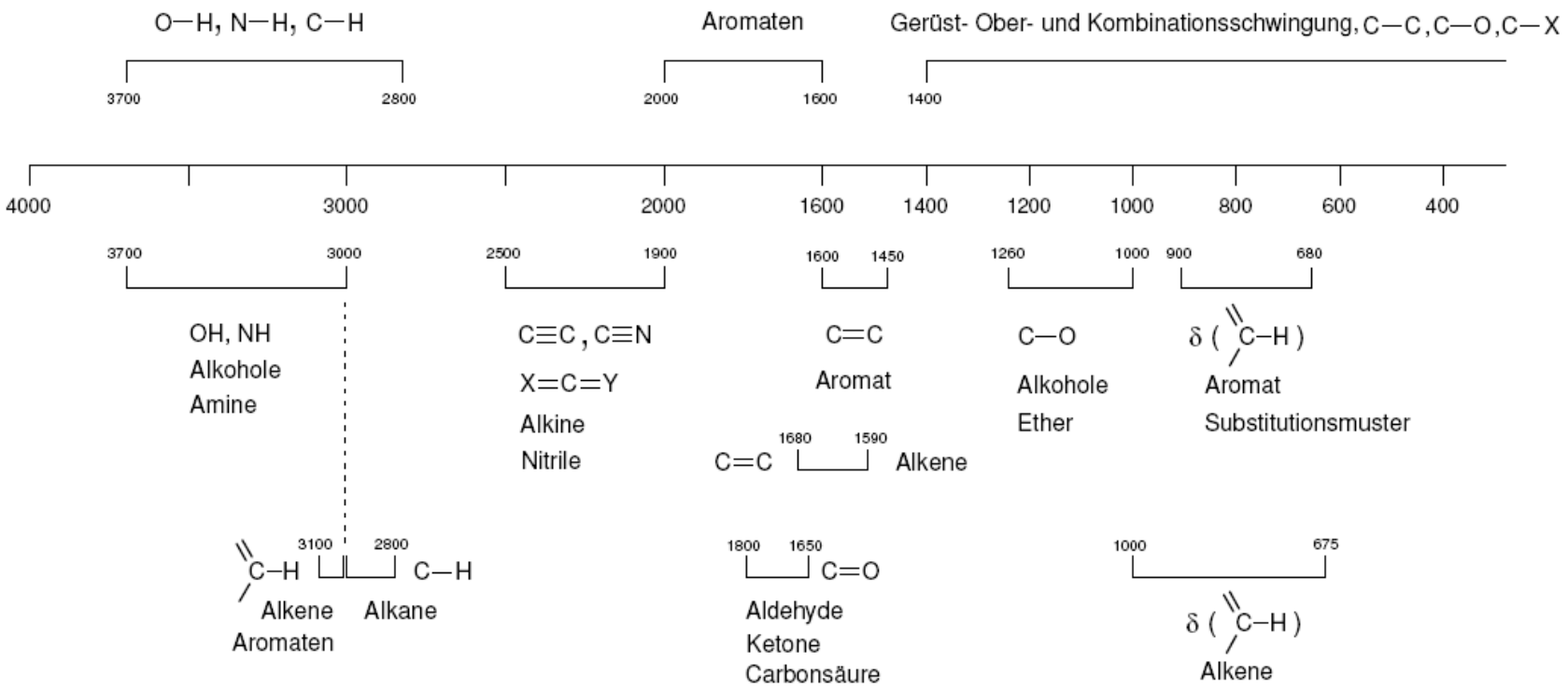

Fundamentals – harmonic oscillator

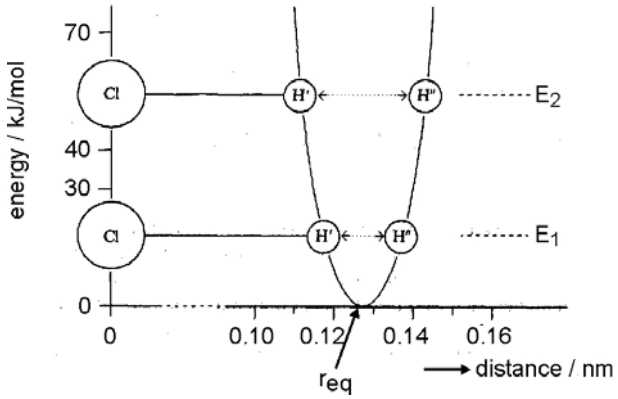

$$F = -(dV/dx) = -k(r - r_{eq})$$

$$V = k(r - r_{eq})^2$$

$$\nu = \frac{1}{2\pi}(k/\mu)^{0.5}$$

F…force
V…potential energy
k…force constant

μ…reduced mass
$= m_1 m_2/(m_1+m_2)$

solving the Schrödinger equation for the harmonic oscillator yields:

$$E_v = (v + \tfrac{1}{2})h\nu$$

v … vibrational quantum number

zero-point energy $E_0 = \frac{1}{2}h\nu$

selection rule for harmonic oscillator: $\Delta v = \pm 1$

in order to be infrared active, the dipole moment must change during a vibration.

$(d\mu/dr) \neq 0$

Harmonic approximation is only valid for small deviations from the equilibrium position.
Shortcoming: bond can not break!

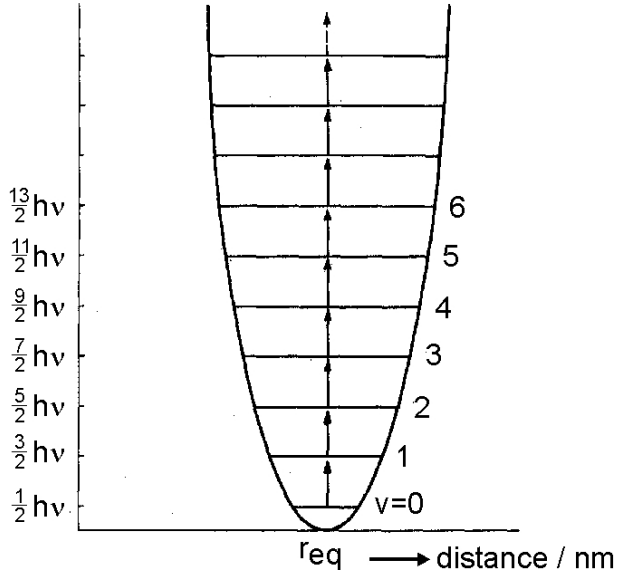

Fundamentals – anharmonic oscillator

a physically more realistic potential:

the Morse potential:

$$V(r) = D(1 - \exp(-a(r - r_{eq})))^2$$

D…dissociation energy

$$E_v = (v + \tfrac{1}{2})h\nu - (v + \tfrac{1}{2})^2 h\nu x_e$$

x_e…anharmonicity constant

Energy levels are no longer equally spaced

selection rule for anharmonic oscillator: $\Delta v = \pm 1, \pm 2, ..$

overtones are allowed
e.g. CO: $v_0 \rightarrow v_1 = 2143\ cm^{-1}$, $v_1 \rightarrow v_2 = 4260\ cm^{-1}$

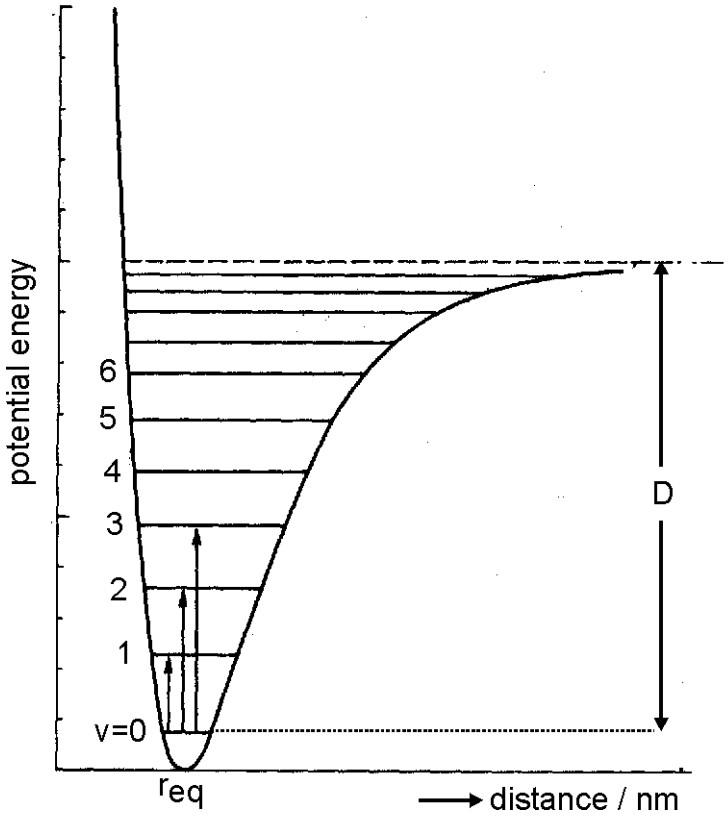

Polyatomic molecules

non-linear molecule: 3N-6 vibrational degrees of freedom

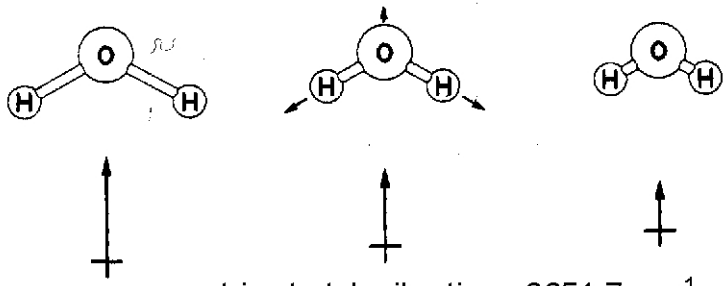

ν_1 symmetric stretch vibration 3651.7 cm^{-1}

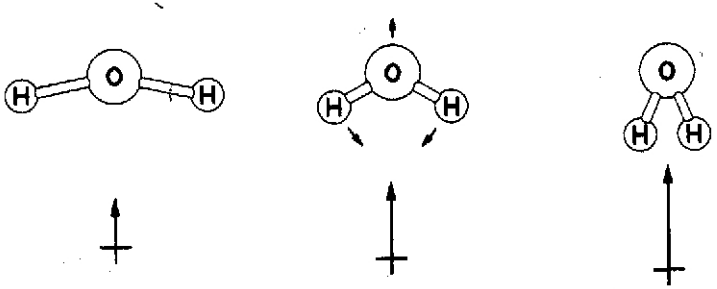

ν_2 deformation (bending) 1595.0 cm^{-1}

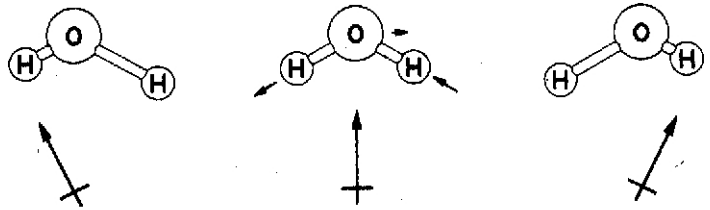

ν_3 anti-symmetric stretch vibration 3755.8 cm^{-1}

linear molecule: 3N-5

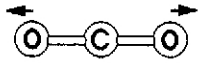

ν_1 symmetric stretch vibration
3651.7 cm^{-1}
IR inactive

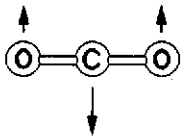

ν_2 deformation (bending)
667.3 cm^{-1}
IR active
degenerate

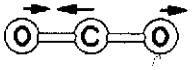

ν_1 anti-symmetric stretch vibration
2349.1 cm^{-1}
IR active

Vibration-rotation spectra

$E(v,J) = (v+\frac{1}{2})h\nu - (v+\frac{1}{2})^2 h\nu x_e + \ldots$
$+ BJ(J+1)$

selection rules for combined vibration/rotation:

two-atomic molecules:
$\Delta v = \pm 1, \pm 2, \ldots \quad \Delta J = \pm 1$

poly-atomic molecules:
for linear molecules $\Delta J = 0$ allowed if the change in dipole moment is perpendicular to the highest symmetric rotational axis.

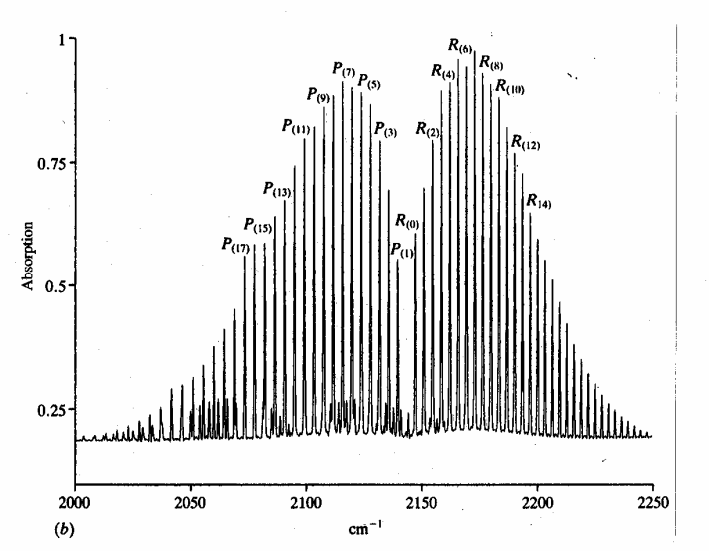

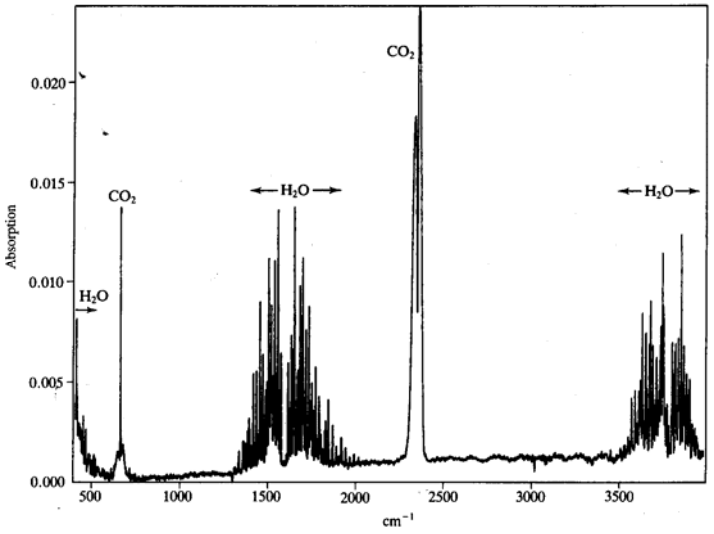

…from the gas-phase to the surface

the rotational freedom is lost and is translated to vibrational modes!

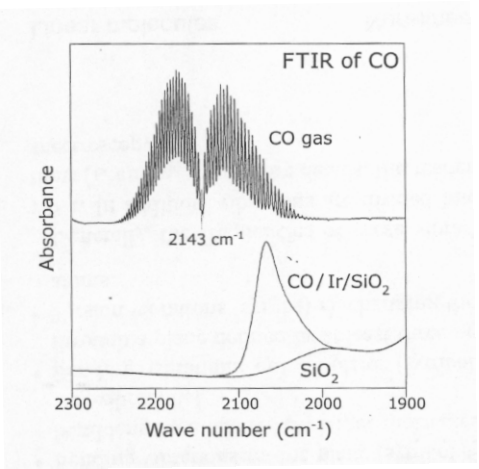

e.g. CO adsorbed on a metal

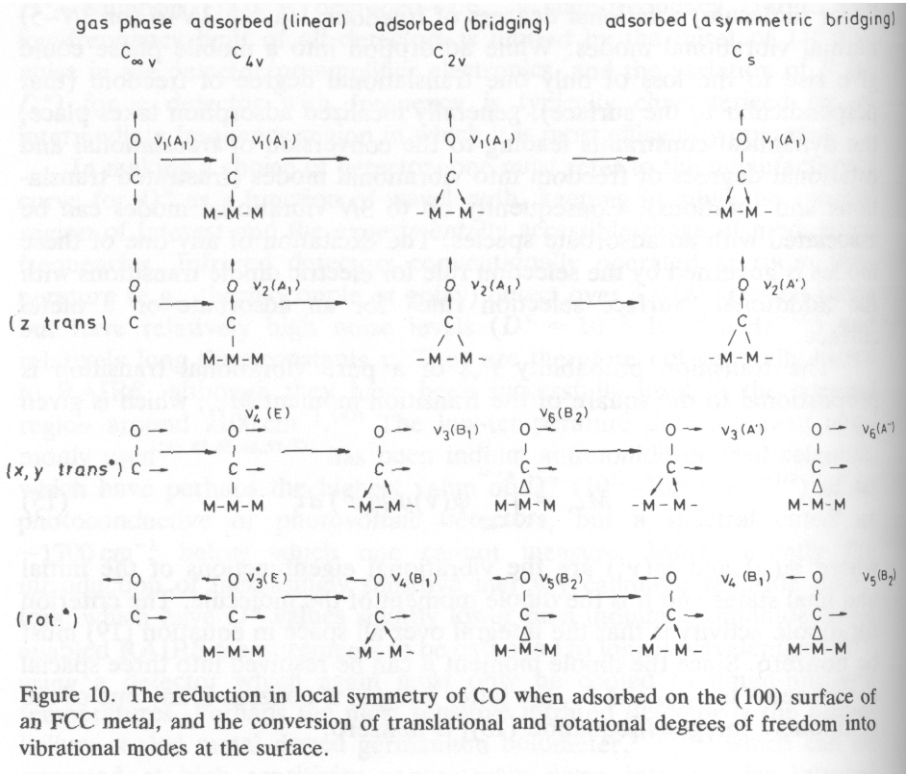

Figure 10. The reduction in local symmetry of CO when adsorbed on the (100) surface of an FCC metal, and the conversion of translational and rotational degrees of freedom into vibrational modes at the surface.

e.g. H_2O adsorbed on a metal

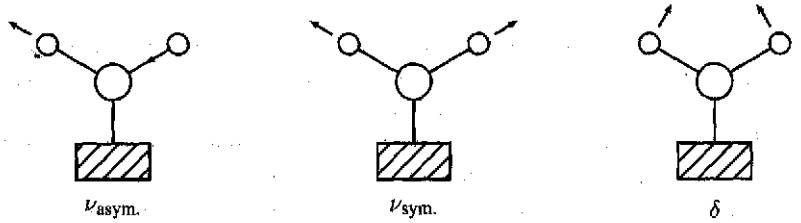

normal modes

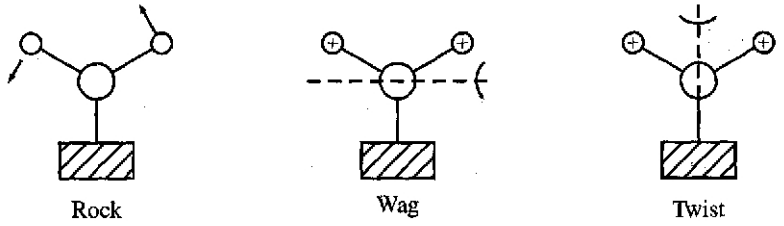

hindered: usually low frequency

ways to obtain information about vibrational properties of adsorbates on surfaces

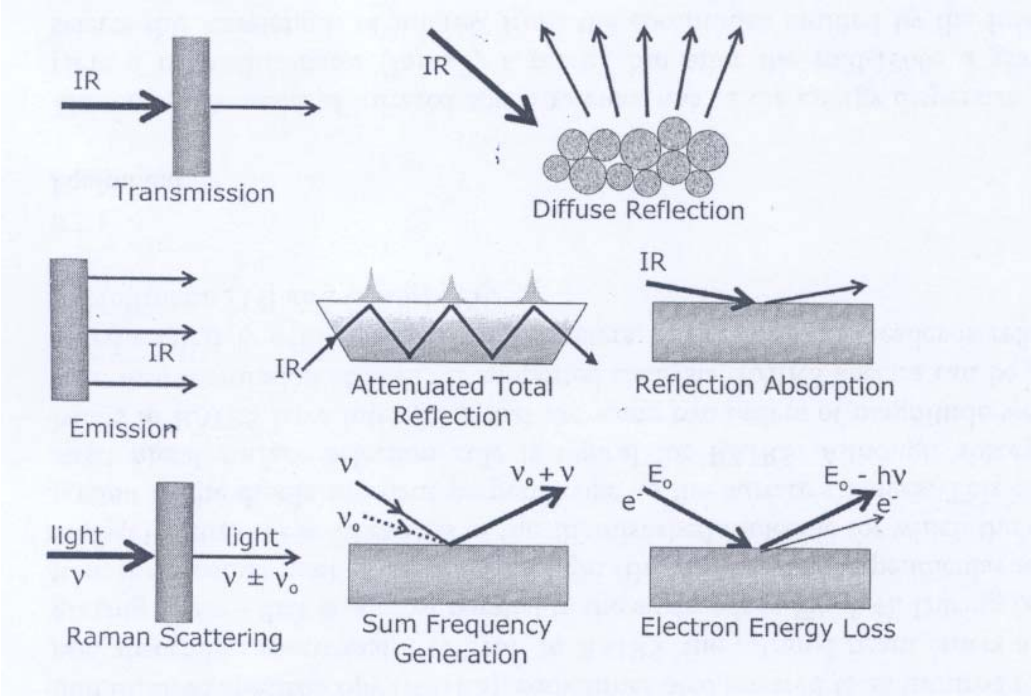

different mechanisms: - absorption of IR photons
- inelastic scattering of photons
- inelastic scattering of electrons
- inelastic scattering of atoms
- inelastic electron tunneling

IR spectroscopy – Instrumentation

Dispersive spectrometers: using monochromator to select the IR wavelength

Standard: Fourier-transform IR spectrometer

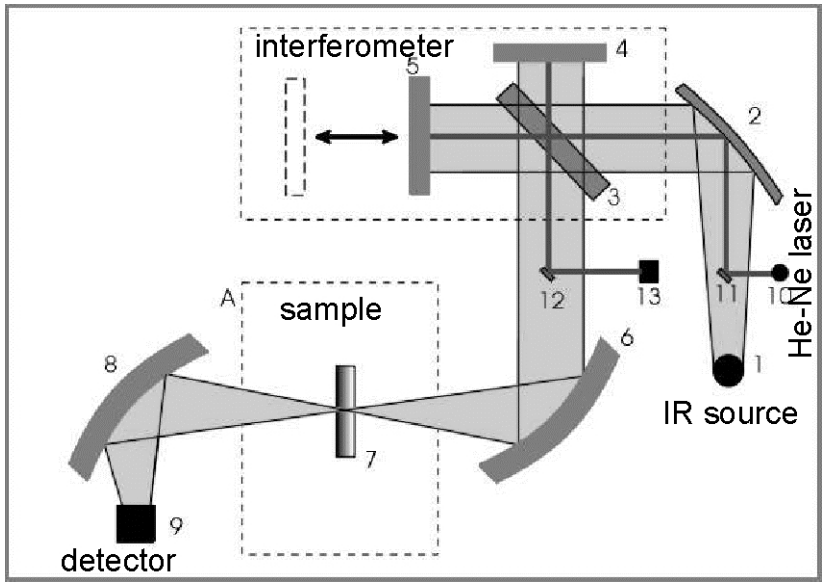

Advantages of FT spectroscopy:

high transmittance (no narrow slits)

multiplex (all frequencies detected simultaneously

IR sources:

Globar: conductive SiC ceramic T = 1200°C

Ni-Cr filament T = 1000-1100°C

Nernst-glower: mixture of oxides (Zr, Y, Er)
T= 1500-2000°C

detectors:

mercury cadmium telluride (MCT) semiconductor

deuterium triglycine sulphate (DTGS) = thermal detector (heat sensing element)

optical components:

NaCl (650 – 4000 cm^{-1})

KBr (400 – 4000 cm-1)

CsJ (200 – 4000 cm-1)

methods:

Transmission IR

Diffuse Reflectance IR

Reflection-Absorption IR

Beer-Lambert law: transmittance $T(I) = I/I_0$

absorbance $A(I) = - \log T(I)$

measure a sample and a reference spectrum

Interferometry

Michelson interferometer

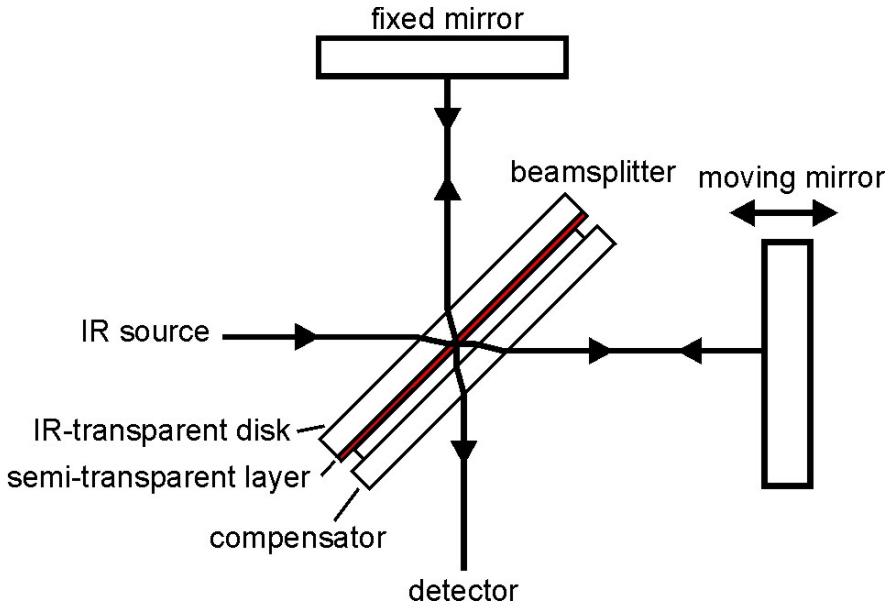

monochromatic source

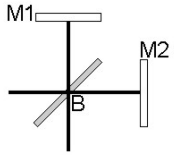

e.g. $\overline{BM2} = \overline{BM1} + n\lambda/2$ (n=0,1,2,..) retardation = $n\lambda$

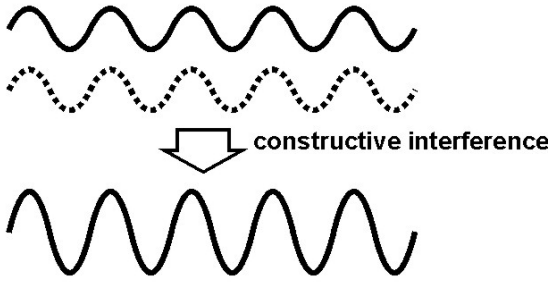

e.g. $\overline{BM2} = \overline{BM1} + \lambda/4$, retardation = $\lambda/2$

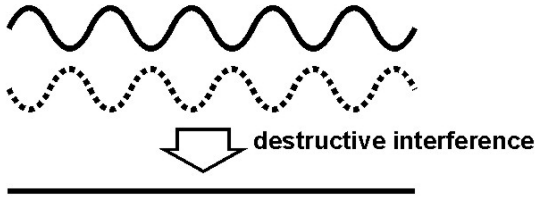

detector signal

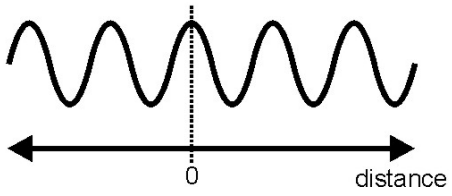

Interferogram and Fourier transformation – monochromatic source

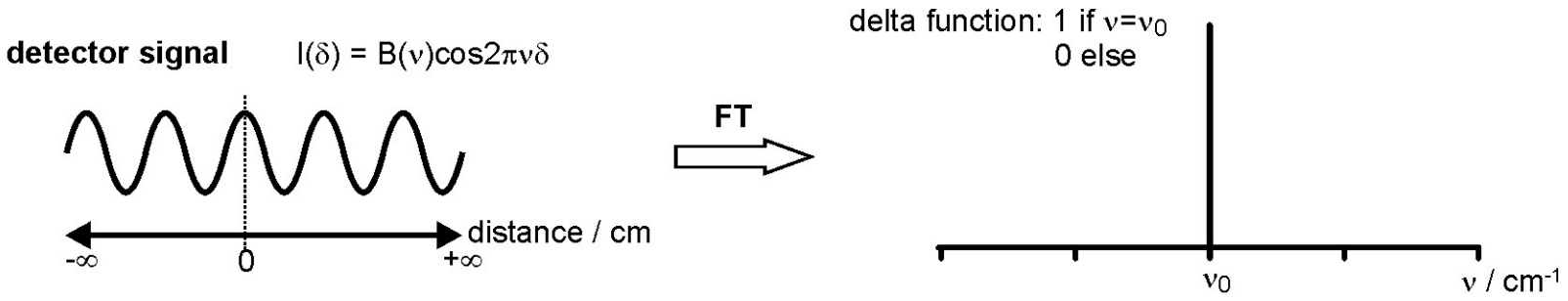

however: the interferometer cannot be displaced to infinite distance

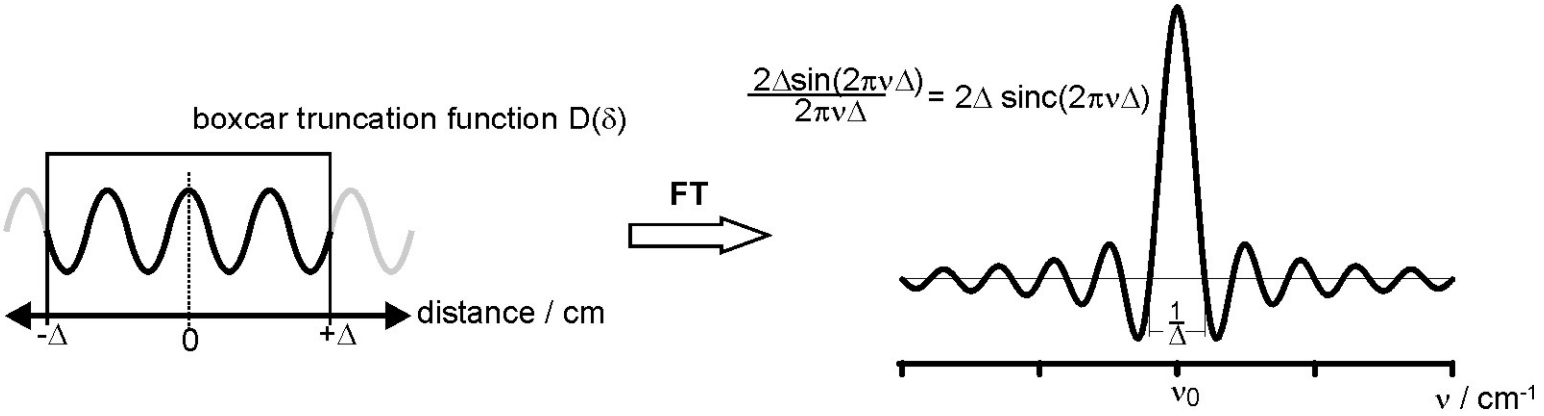

⇨ resolution of the interferometer (approx.): $\Delta\nu = (\Delta_{max})^{-1}$

⇨ distorted line shape - is corrected by APODIZATION
(using different weighting functions)

Interferogram and Fourier transformation – polychromatic source

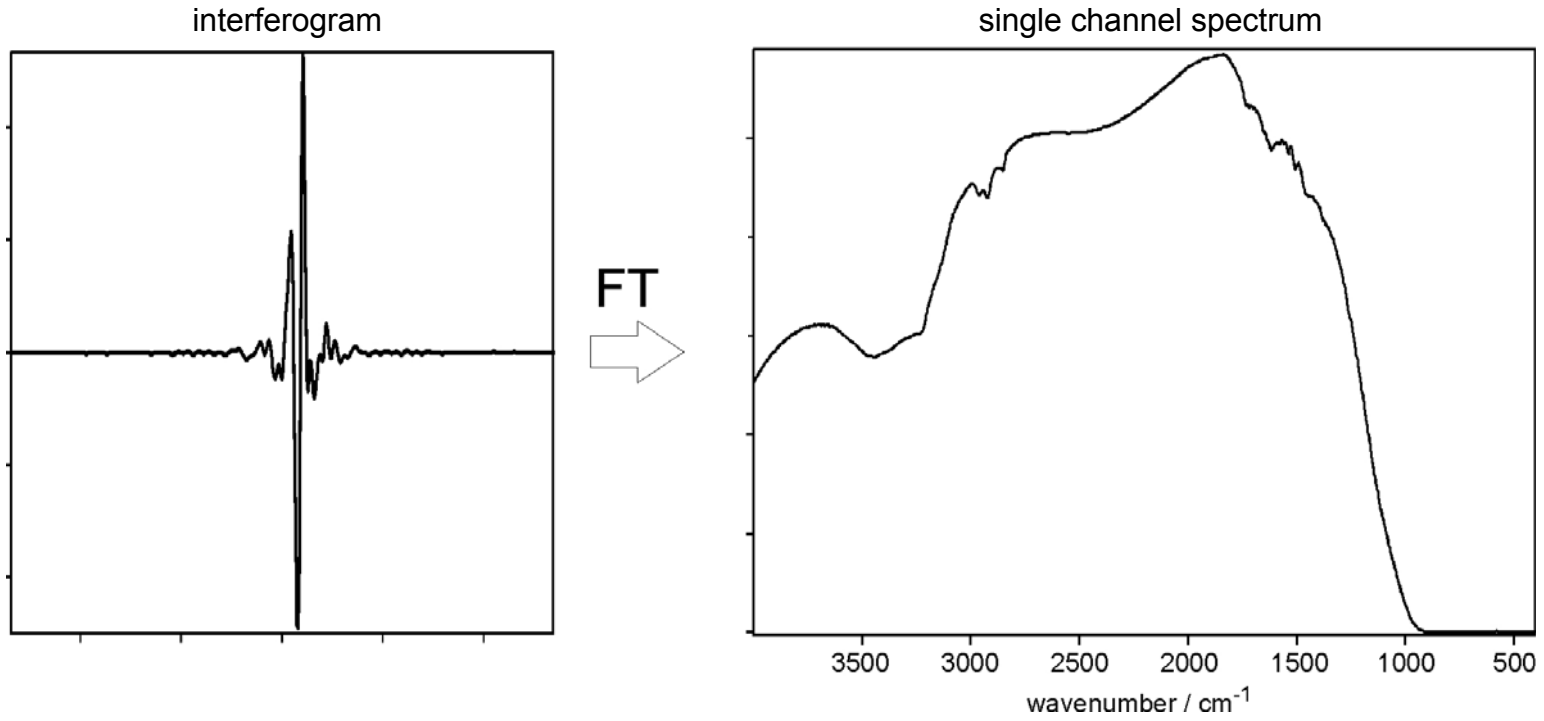

single channel spectrum contains thermal emission characteristics of the light source, absorption of optical elements, and absorption by the sample.

therefore: divide by single channel reference spectrum

Transmission IR spectroscopy

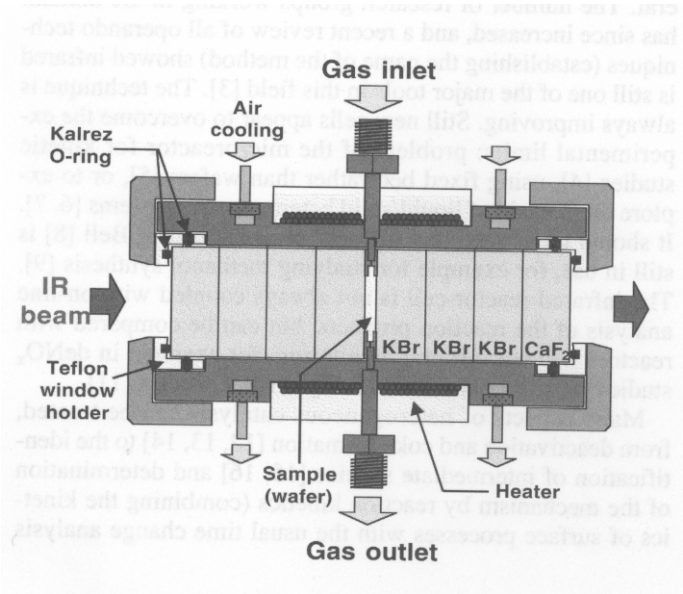

Transmission IR cell

example: dehydroxylation of MgO powder

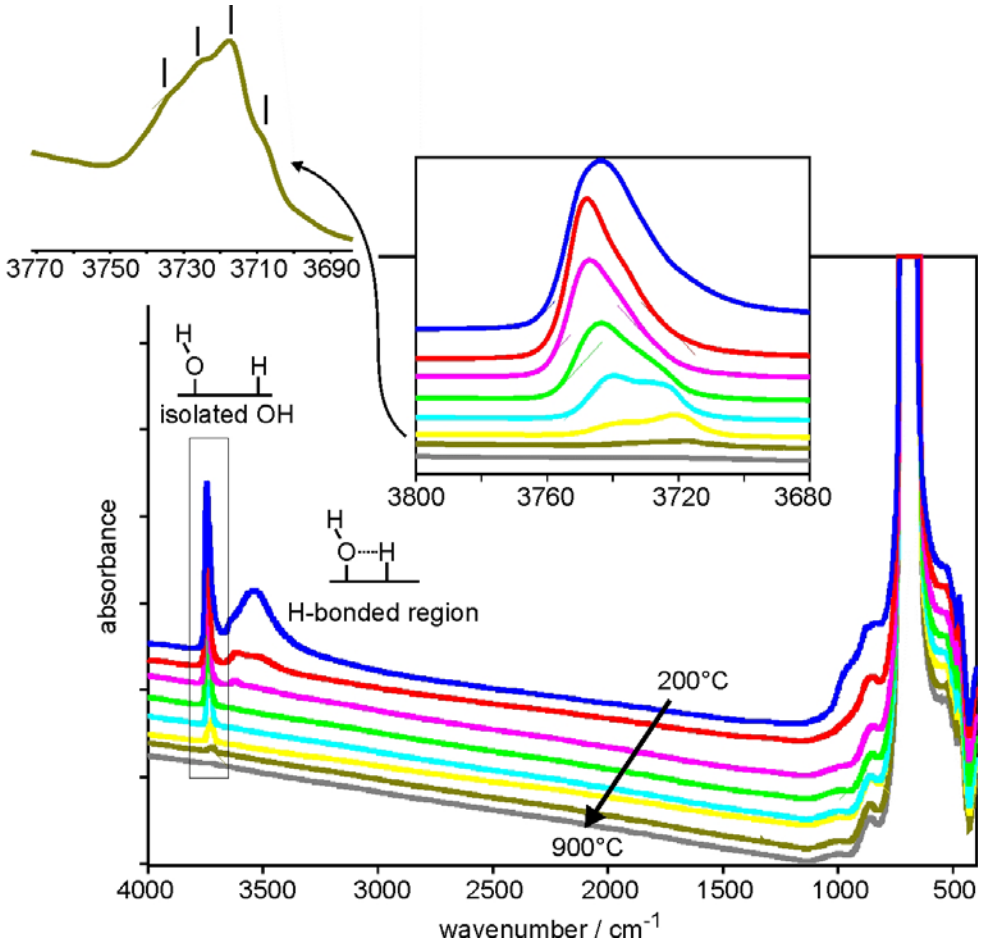

Diffuse reflectance infrared spectroscopy (DRIFTS)

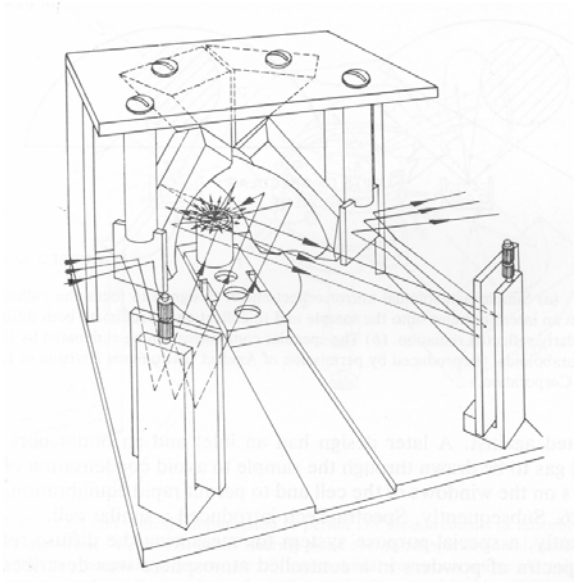

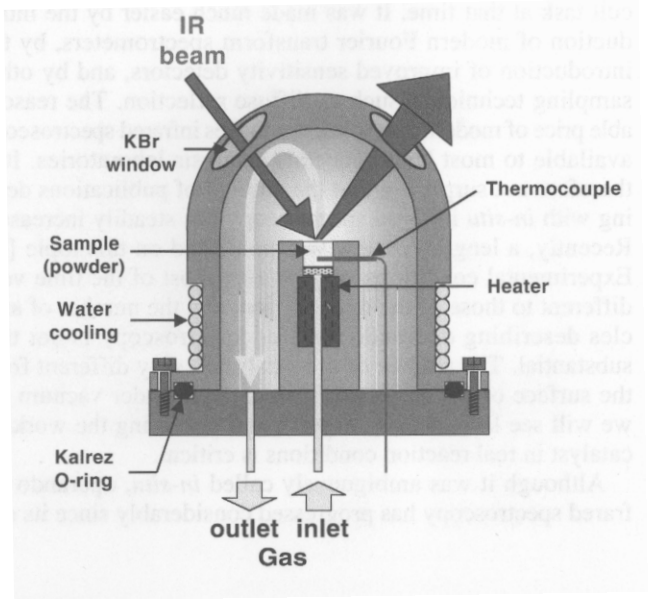

specular reflection

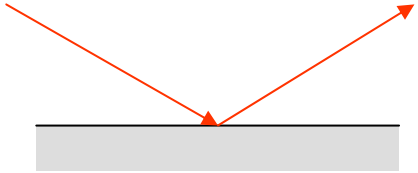

diffuse reflection

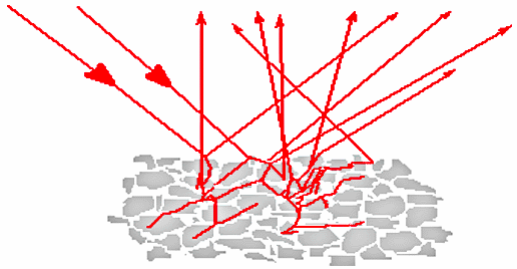

Beer-Lambert law not valid

In a diffuse reflectance experiment, the phenomena of absorption and scattering are always observed at the same time. A model to separate these two effects from each other was developed by Kubelka and Munk. Their theory shows, that the remittance of a sample depends only on the ratio between the coefficients of absorbance and scattering, but not on their absolute values. By assuming the scattering coefficient to be constant in a given energy range, the Kubelka-Munk model allows to derive an absorbance spectrum from the respective reflectance spectrum. The positions of reflectance minima correspond to the maxima of absorption of the sample.

$$\frac{k}{s} = \frac{(1-R_\infty)^2}{2R_\infty}$$

temperature gradient between surface and bottom of cup
large dead volume (strong gas-phase absorption)

Attenuated total internal reflection infrared spectroscopy (ATR-IR)

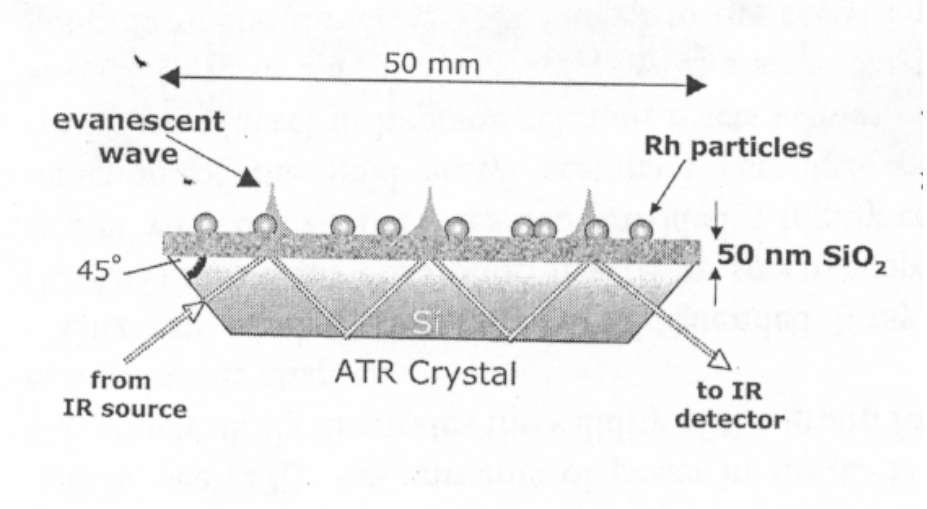

Total internal reflection occurs when light is incident on a medium Boundary at an angle larger than the critical angle.

$$\theta_c = \arcsin(n_2/n_1)$$

Light travelling from medium with higher refractive index (n_1) to the one with low refractive index (n_2)

An exponentially decaying evanescent wave penetrates into the less dense medium.

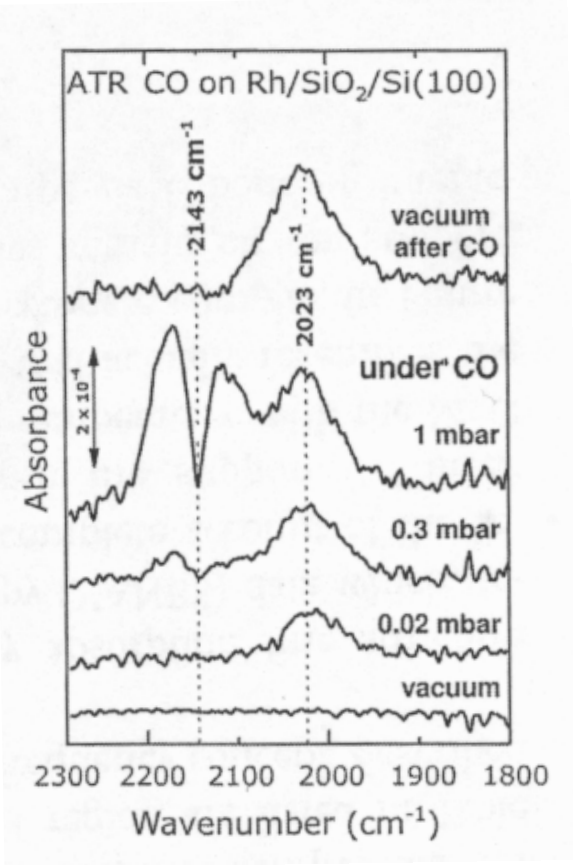

Infrared reflection absorption spectroscopy – IRAS

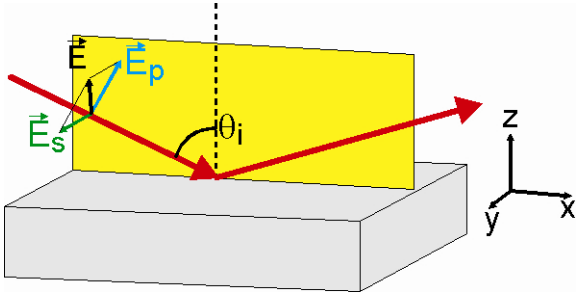

the phase of the light shifts upon reflection!

the phase of s-polarized light is shifted by 180°, independent of the angle of incidence.

the phase shift of p-polarized light depends on the angle of incidence.

Two limiting polaization states of the IR electric field vector:
E_p: parallel to the plane of incidence
E_s: perpedicular to the plane of incidence

$$E_y^{\text{vacuum}}(z=0) = \left[1 - \frac{(\tilde{\epsilon} - \sin^2\theta)^{1/2} - \cos\theta}{(\tilde{\epsilon} - \sin^2\theta)^{1/2} + \cos\theta}\right] E^0$$

$$E_x^{\text{vacuum}}(z=0) = \left[1 - \frac{\tilde{\epsilon}\cos\theta - (\tilde{\epsilon} - \sin^2\theta)^{1/2}}{\tilde{\epsilon}\cos\theta + (\tilde{\epsilon} - \sin^2\theta)^{1/2}}\right] (\cos\theta\, E^0)$$

$$E_z^{\text{vacuum}}(z=0) = \left[1 + \frac{\tilde{\epsilon}\cos\theta - (\tilde{\epsilon} - \sin^2\theta)^{1/2}}{\tilde{\epsilon}\cos\theta + (\tilde{\epsilon} - \sin^2\theta)^{1/2}}\right] (\sin\theta\, E^0)$$

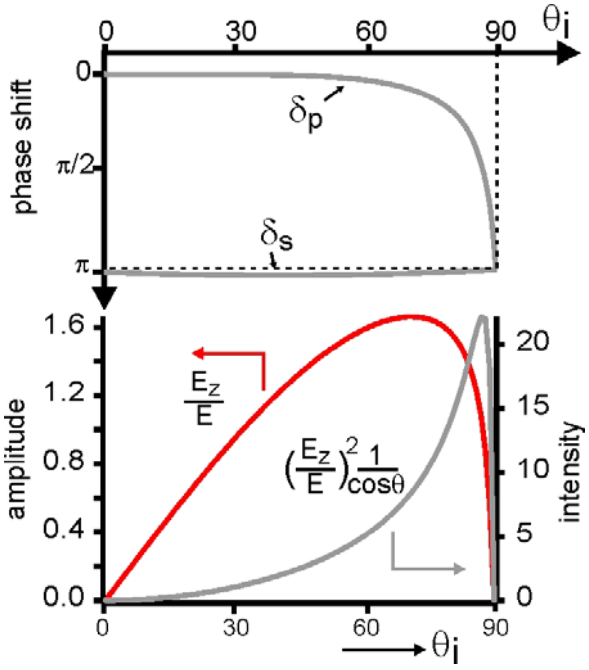

at the metal surface:
electric field **enhancement** (constuctive interference between incident and reflected radiation) for **p-polarized** light at grazing incidence
electric field **cancellation** (destructive interference between incident and reflected radiation) for **s-polarized** light at all angles of incidence.

only the p-polarized part of the IR radiation may interact with dipoles on the surface.

Infrared reflection absorption spectroscopy – IRAS

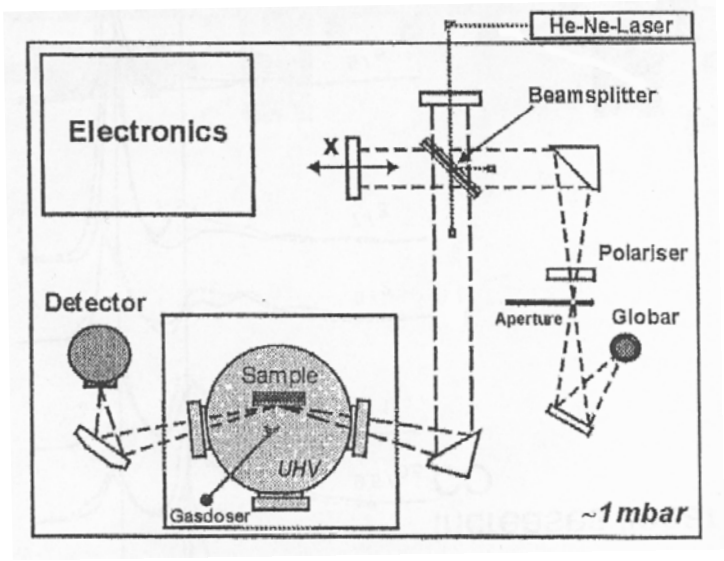

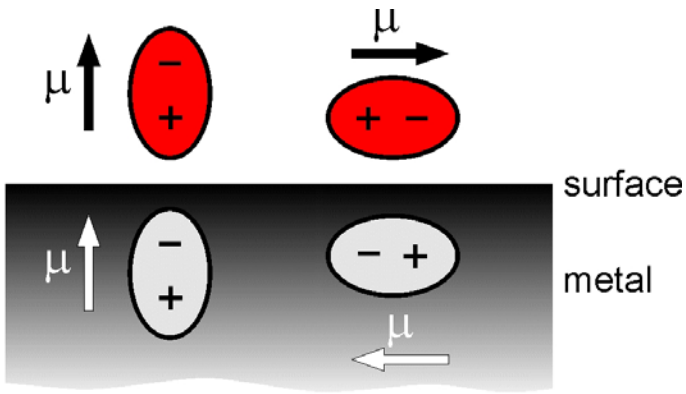

Surface selection rule:
When a molecule is adsorbed on a metallic substrate, the molecule induces opposite image charges in the substrate. The dipole moment of the molecule and the image charges perpendicular to the surface reinforce each other. In contrast, the dipole moments of the molecule and the image charges parallel to the surface cancel out.
Therefore, only molecular vibrational modes giving rise to a dynamic dipole moment perpendicular to the surface will be observed in the vibrational spectrum.

Infrared reflection absorption spectroscopy – IRAS

example: CO adsorption on thin MgO films, probing surface heterogeneity

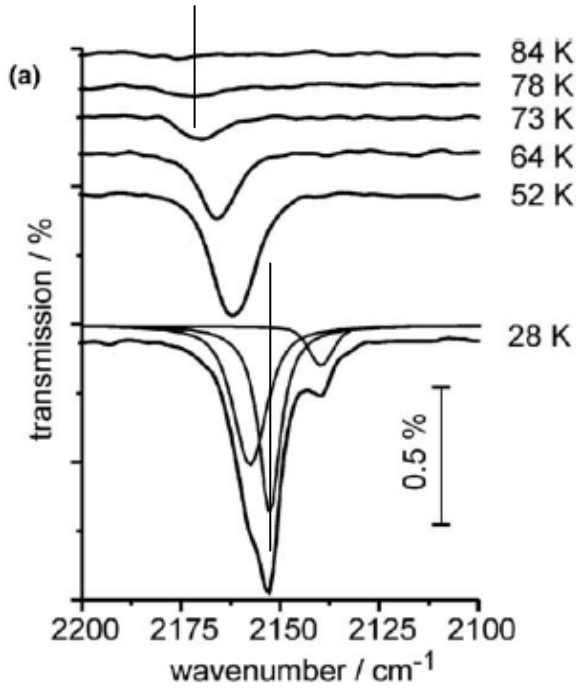

low coverage

strong binding sites are populated first

2170 cm^{-1}, defects, low-coordinated sites

full coverage

2152 cm^{-1}, CO on the regular surface

Infrared reflection absorption spectroscopy – IRAS

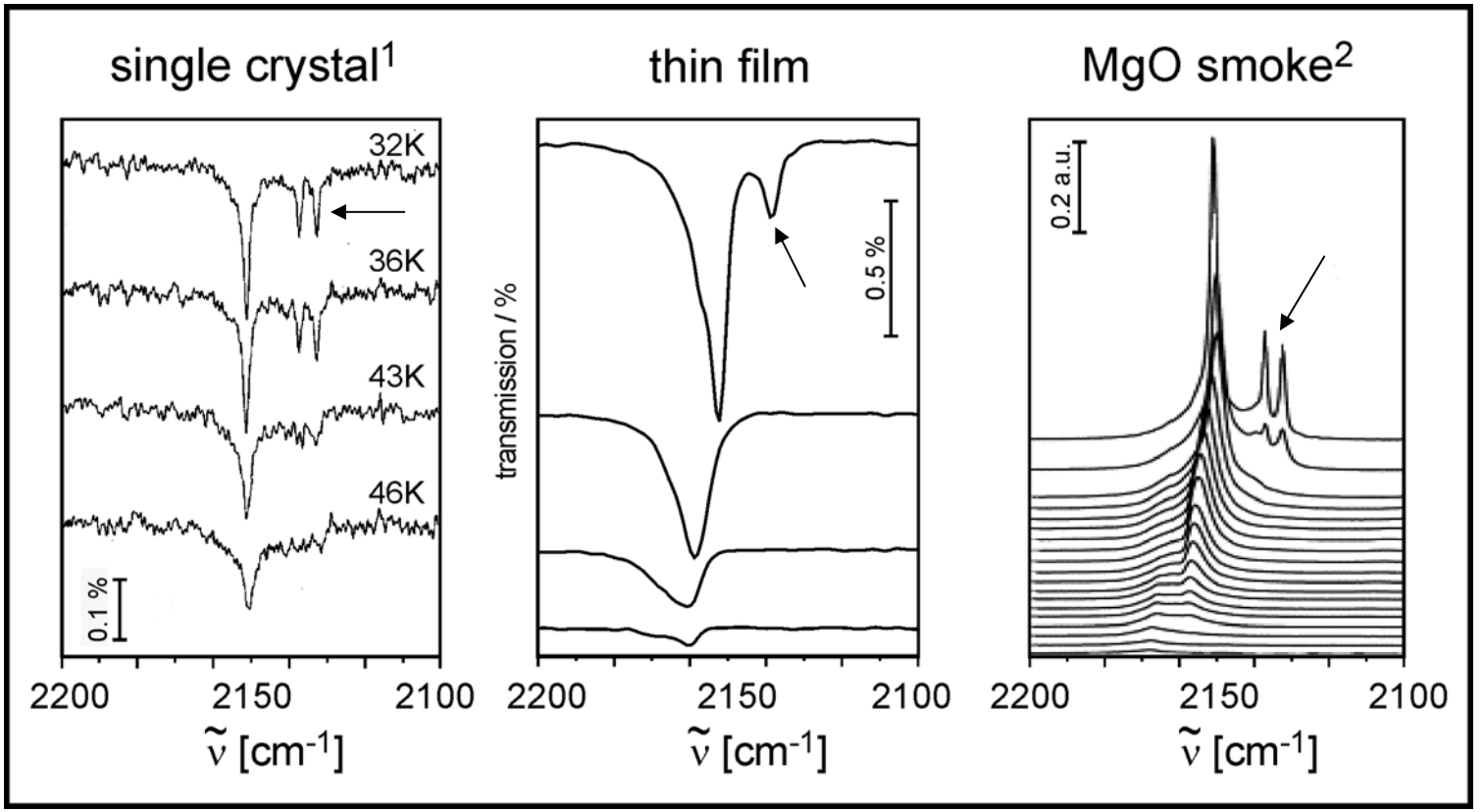

Two tilted CO in the unit cell at full coverage CO on MgO

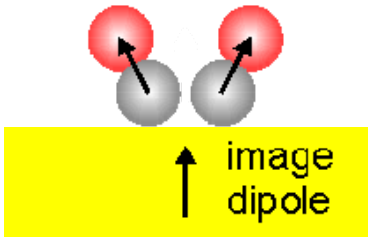

due to the surface selection rule only the perpendicular component can be detect on the thin film sample

Infrared reflection absorption spectroscopy – IRAS

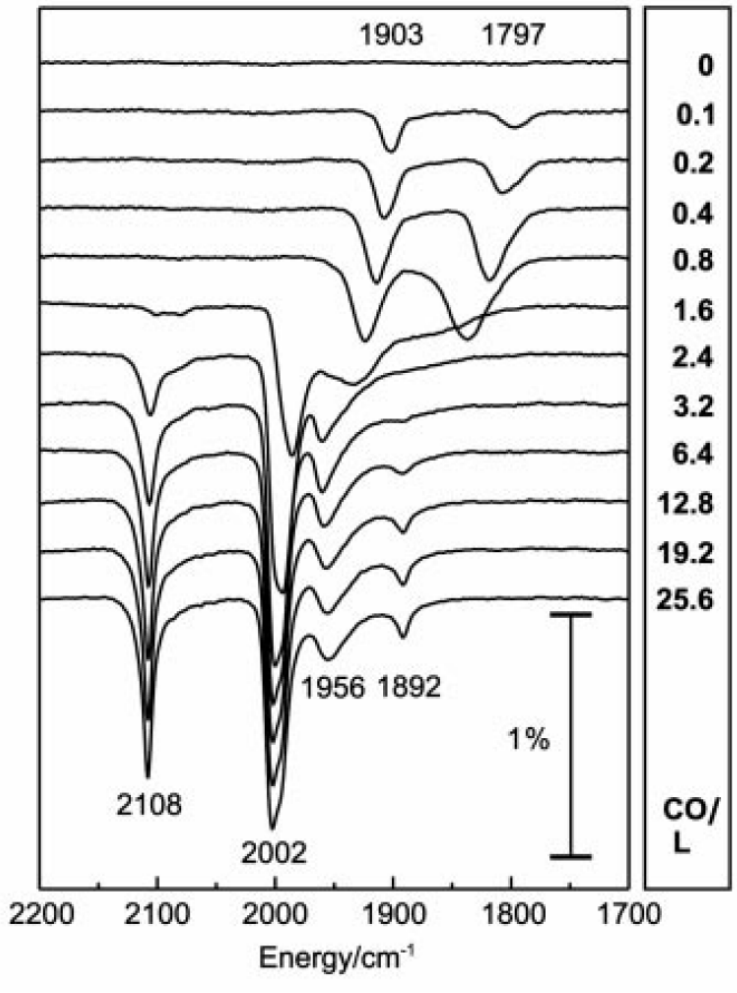

M. Frank and M. Bäumer, PCCP **2**, 3723 (2000).

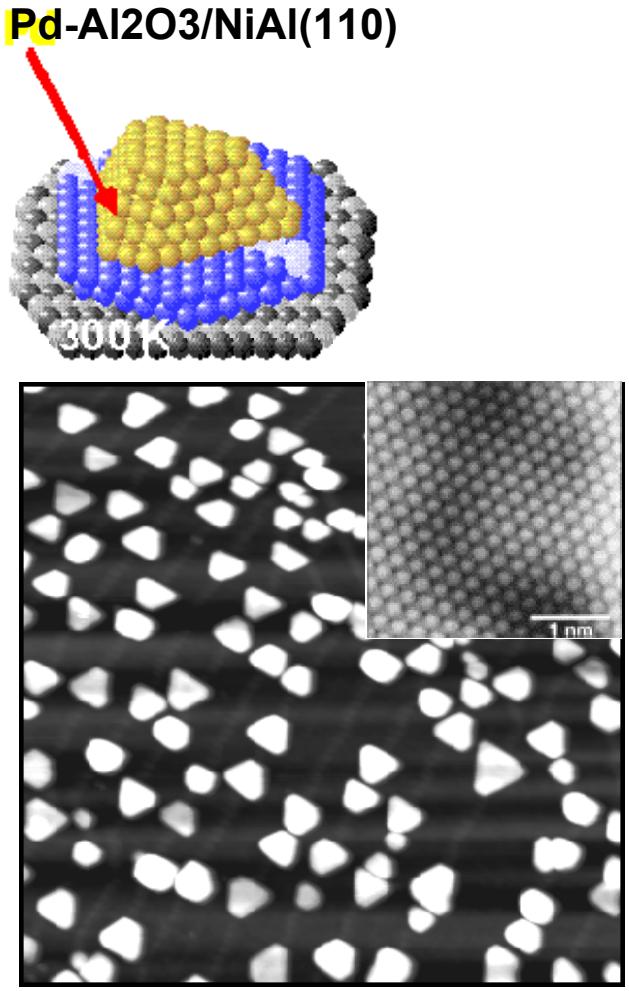

K. H. Hansen *et al.* Phys. Rev. Lett. **83**, 4120 (1999).

Infrared reflection absorption spectroscopy – IRAS

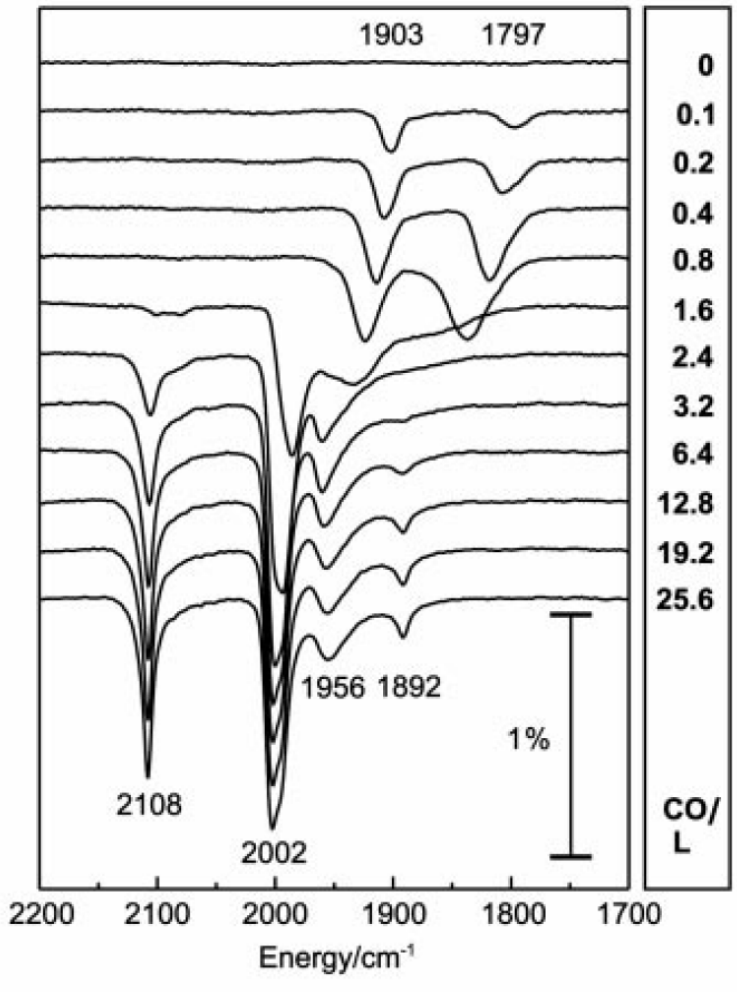

CO stretching frequency is a measure for the metal electron density.

		CO stretching frequency
gas-phase	C–O	2143 cm^{-1}
on-top	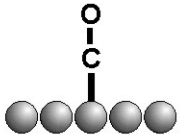	2120 - 1920 cm^{-1}
bridge	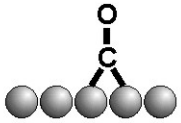	1920 - 1800 cm^{-1}
3-fold hollow	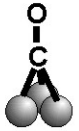	<1800 cm^{-1}

Blyholder model

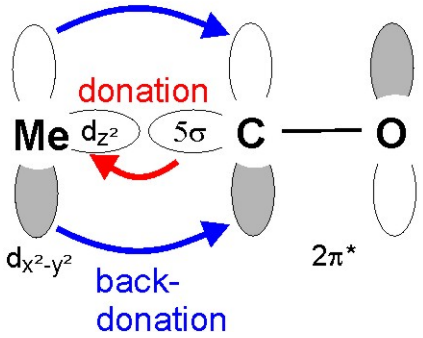

Polarization modulation infrared reflection absorption spectroscopy – PM-IRAS

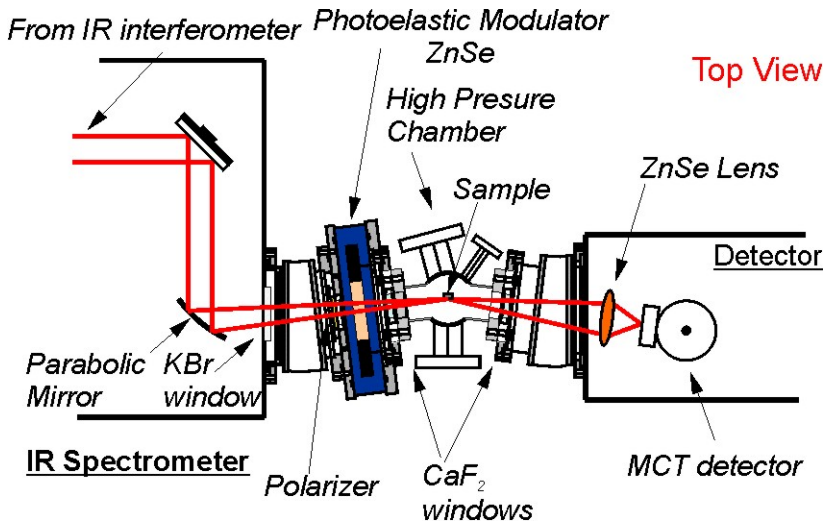

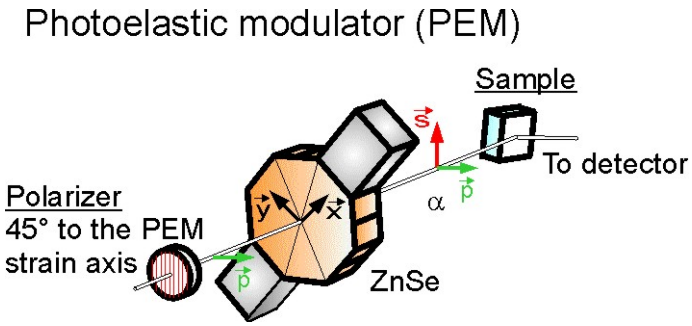

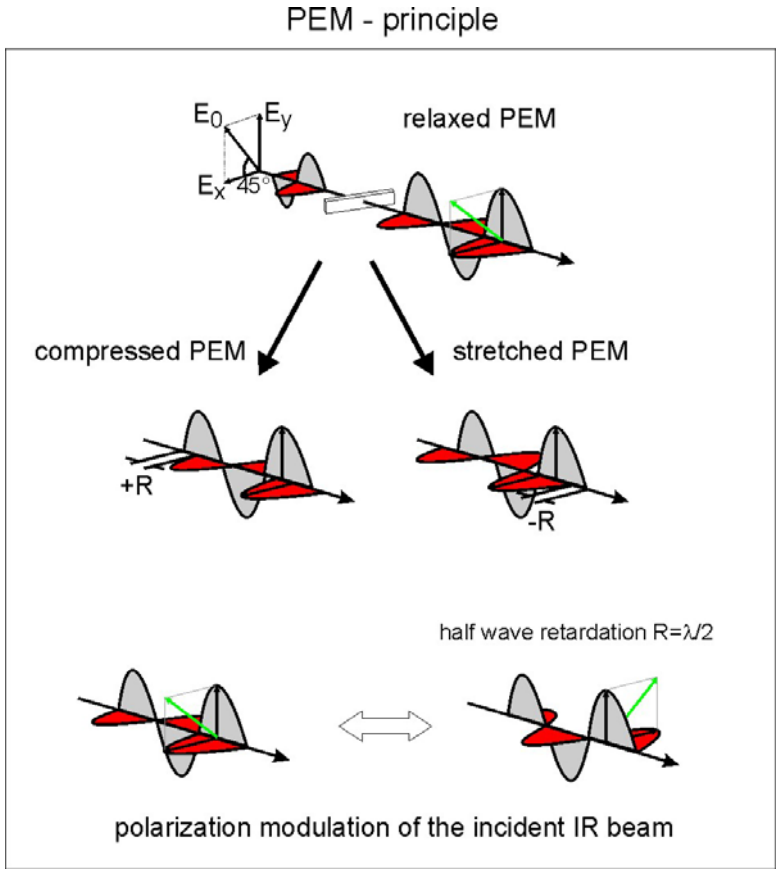

Surface selection rule: vanishing electric field of the s-polarized component at a metal surface.

with **p**-polarized component: detect **gas-phase** + **surface**
with **s**-polarized component: detect **only gas-phase**

Polarization modulation infrared reflection absorption spectroscopy – PM-IRAS

High pressure IRAS **without PEM**:

50 mbar CO on Pd(111)

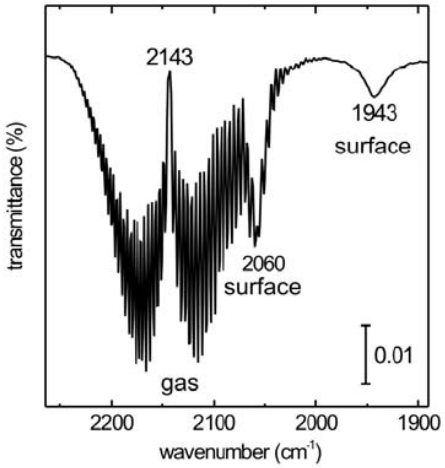

Surface signal partly obscured
by strong gas-phase CO absorption.

High pressure IRAS **with PEM**:

50 mbar CO on Pd(111)

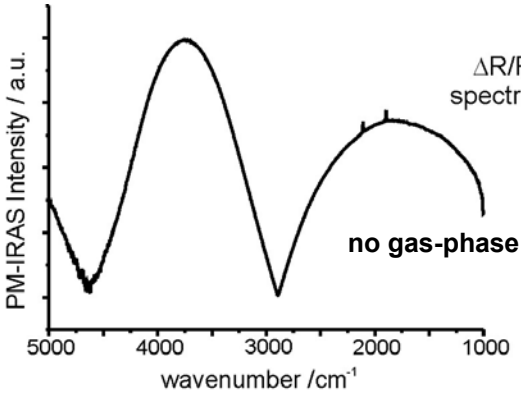

$$\frac{\Delta R}{R} = \frac{I_p - I_s}{I_p + I_s}$$

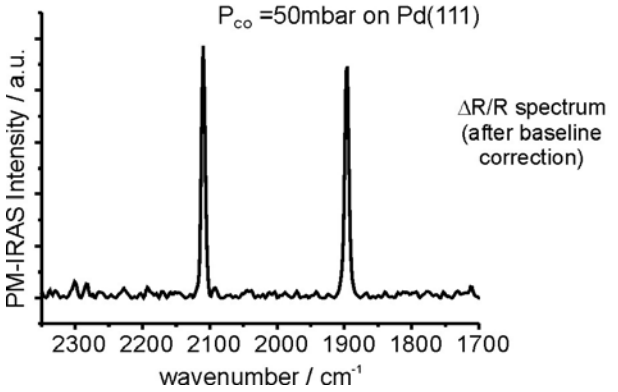

Polarization modulation infrared reflection absorption spectroscopy – PM-IRAS

Example: CO interaction with Au clusters deposited on MgO thin films

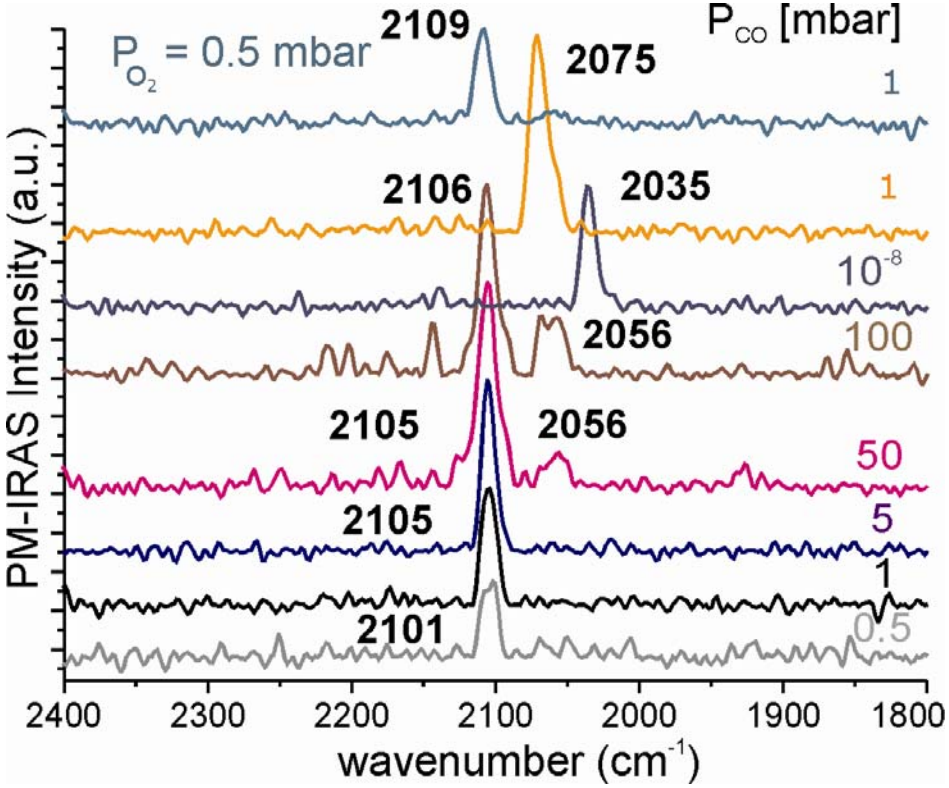

A new line appears during high pressure adsorption

Modification of the Au clusters or support

Oxidation restores the original spectrum

Polarization modulation infrared reflection absorption spectroscopy – PM-IRAS

Example: CH_3OH oxidation on Pd(111), information in the gas-phase spectrum

surface contribution

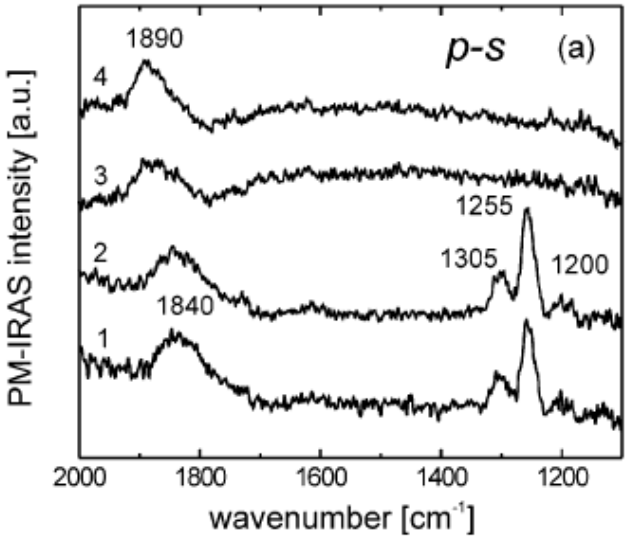

gas-phase contribution

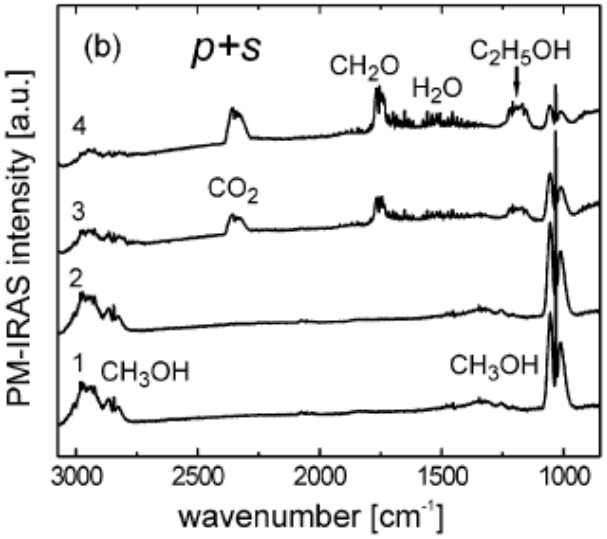

After 60 min.

+CH_3OH + O_2, 400K

+CH_3OH + O_2, 300K

+CH_3OH, 300K

1840 cm^{-1}: CO

1305, 1255 cm^{-1}: formaldehyde

1200 cm^{-1}: formyl

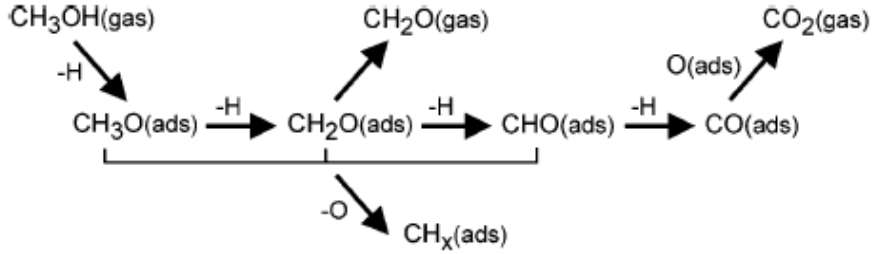

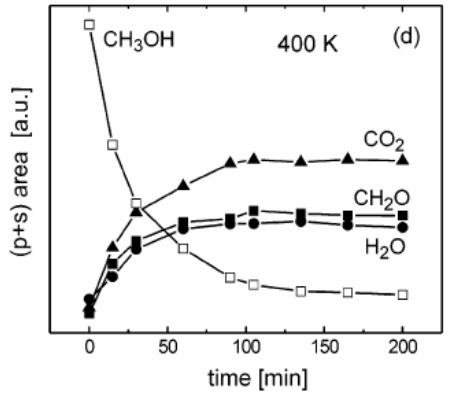

Raman spectroscopy

Inelastic scattering of photons

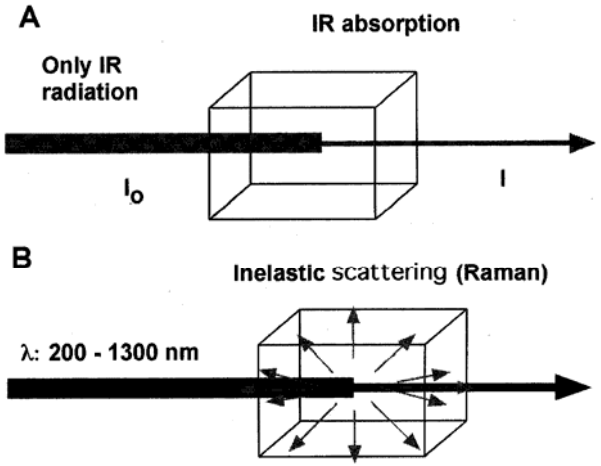

Figure 4. Interaction of the radiation with the matter for IR spectroscopy (A) and for Raman spectroscopy (B).

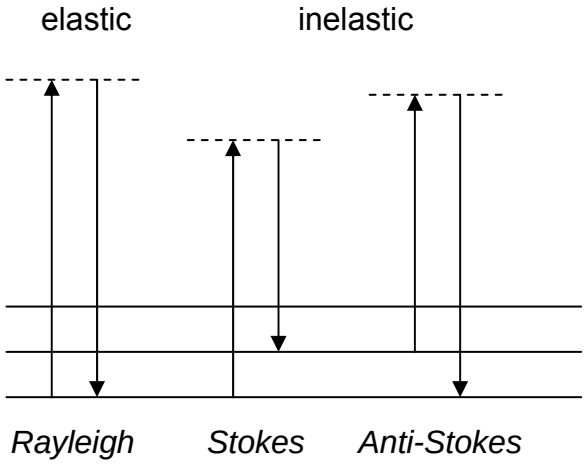

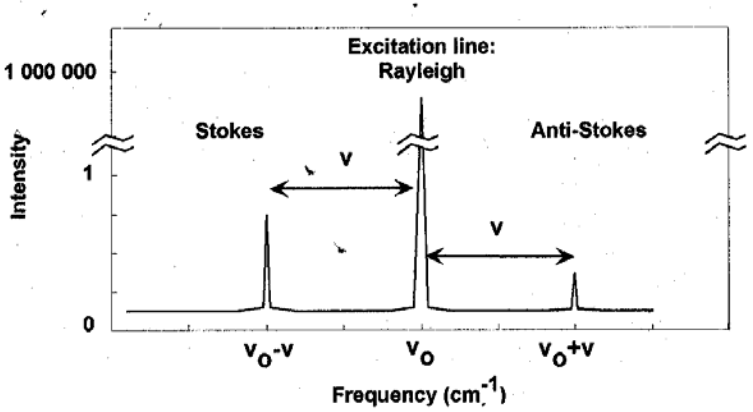

Figure 3. Scattered radiation during Raman spectra, the relative intensities of *Rayleigh, Stokes and anti-Stokes bands is presented qualitatively.*

Raman spectroscopy

Selection rules in Raman spectroscopy:

$\Delta v = \pm 1$

and

change in polarizability α

$(d\alpha/dr) \neq 0$

In general: electron cloud of apolar bonds is stronger polarizable than that of polar bonds.

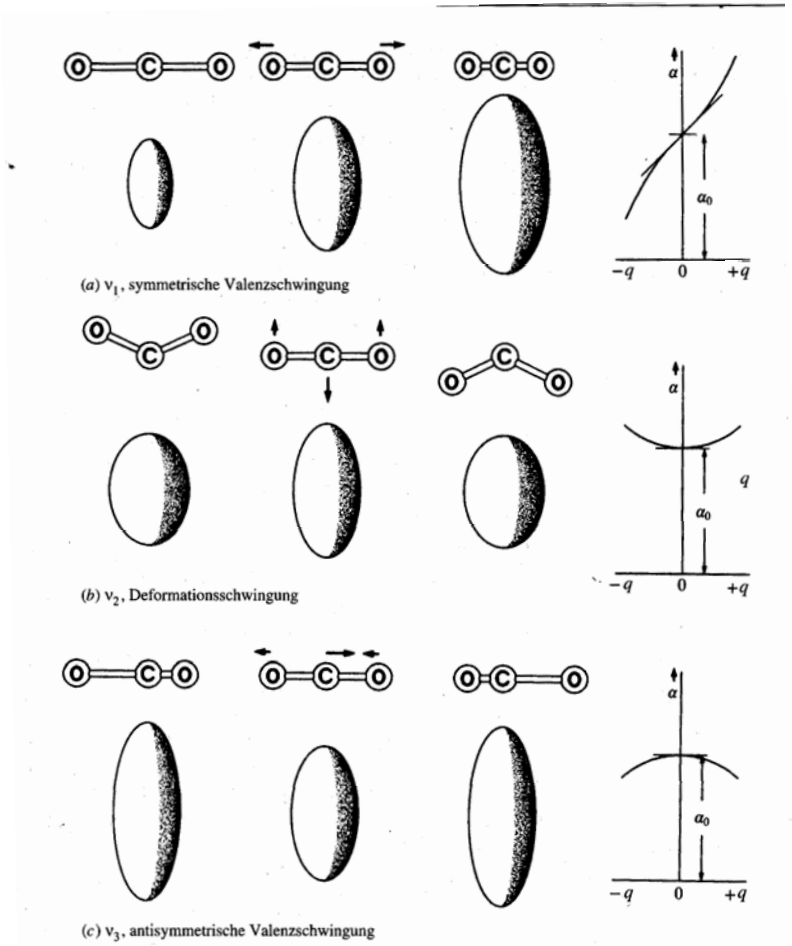

Bild 4.7: Die Änderung des Polarisierbarkeitsellipsoids von Kohlendioxid im Verlauf seiner Schwingungsbewegungen sowie Diagramme, die die Änderung der Polarisierbarkeit α als Funktion der Auslenkungskoordinate q im Verlauf einer jeden Schwingung wiedergeben.

Raman spectroscopy

Advantages of Raman

- wide spectral range 50 – 5000 cm^{-1}
- negligile gas phase scattering
- quartz is a very weak Raman scatterer; cells/windows can be made out of quartz
- can be done also at high temperatures (e.g. 1000 °C) because of detection in the optical regime; no perturbation by blackbody radiation
- catalysis: typical oxide supports (silca, alumina) are weak scatteres

Disadvantages of Raman

- low intrinsic cross section
- susceptible to fluorescence (can be up to 10^6 higher; especially coke has a high fluorescence yield)
- heating due to intense lasers
- quantification of Raman intensities is very diffcult (even with reference samples, because of possible electronic effects of the substrate)

UV-Raman is not affected by fluorescence
however: lower spectral resolution
large energy, sample degradation
detection

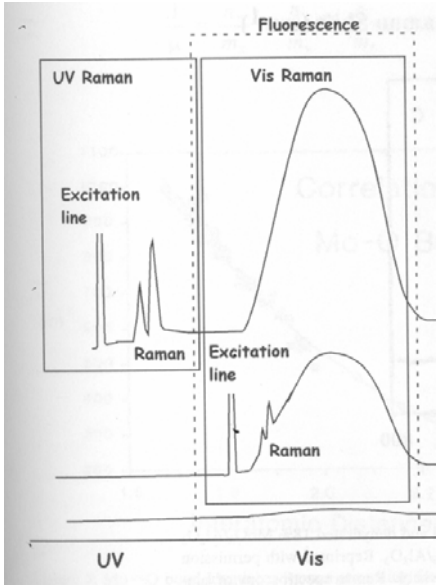

Raman spectroscopy - example

Raman provides insight into structure of oxides, crystallinity, coordination of the metal oxide sites; can also be used as a microprobe and give spatial distribution of phases through a sample.

Molybdena catalysts: hydrotreating and partial oxidation

Prepared by impregnation of the support with a solution of ammonium heptamolybdate $(NH_4)_2Mo_7O_{24}$ 4H2O.

Different Mo-complexes are stable depending on the pH

		pH 4.8-6.8	*< 2.2*	*> 8*
Vibration	$(NH_4)_6Mo_7O_{24} \cdot 4\,H_2O$	$Mo_7O_{24}^{6-}$	$Mo_8O_{26}^{4-}$	MoO_4^{2-}
ν_s (Mo=O)	931	943	965	897
ν_{as} (Mo=O)	879	903	925	837
δ (Mo=O)	354	362	370	317
ν (Mo–O–Mo)		564	860	
δ (Mo–O–Mo)	217	219	230	

sharp peaks for MoO_3/SiO_2
high crystalline character

but broad for MoO_3/Al_2O_3

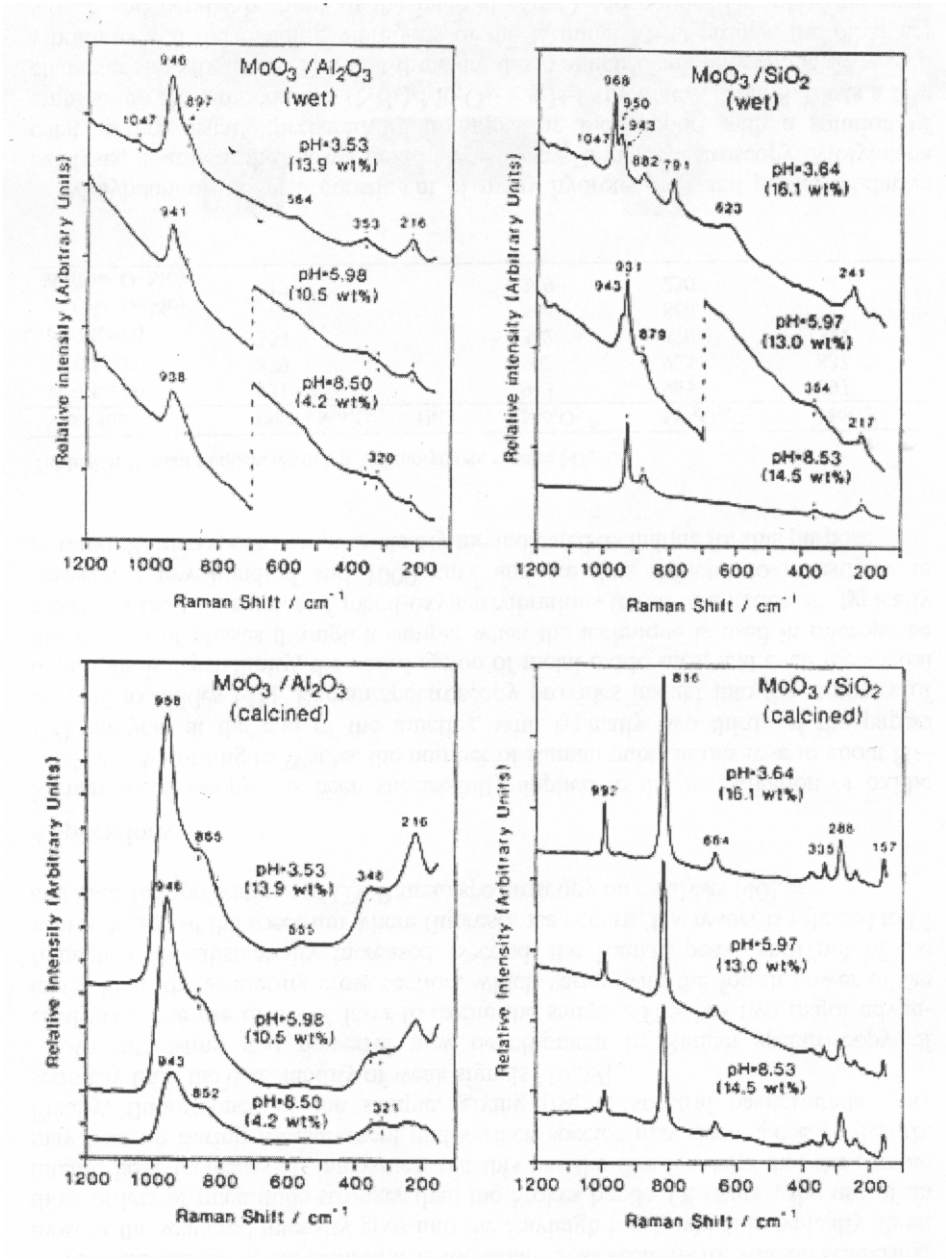

Enhanced Raman spectroscopy

Surface-enhanced Raman spectroscopy:

Surface plasmon resonance: conduction band electrons in the metal surface are excited into an extended surface electronic excited state.
This leads to an enhanced electric field at the surface of the metal.
Adsorbed molecules experience an exceptionally large electromagnetic field.

strong effect for Ag, Au, Cu (plasmon excitation in the VIS).

Intensity of the surface plasmon resonance depends on wavelength of the radiation and the morphology of the surface (roughened surface of small particles)

enhancement factor: ~ 10^7.

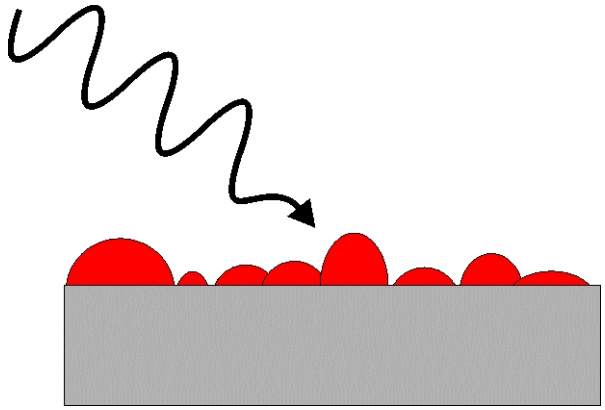

Enhanced Raman spectroscopy

Tip-enhanced enhanced Raman spectroscopy:

combining scanning tunneling microscopy and Raman spectroscopy.
enhancement due to gap modes.
flat surfaces can be investigated.

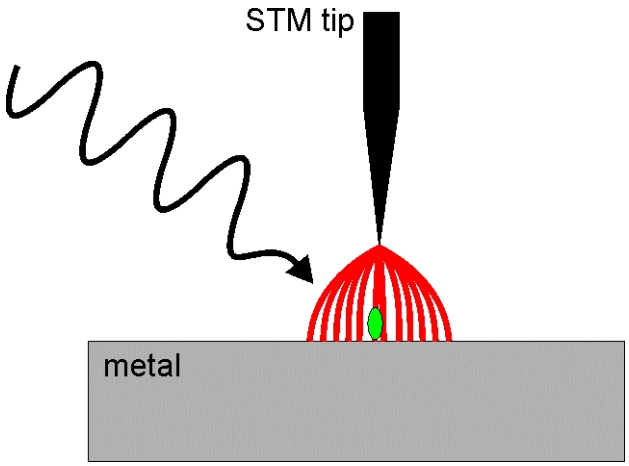

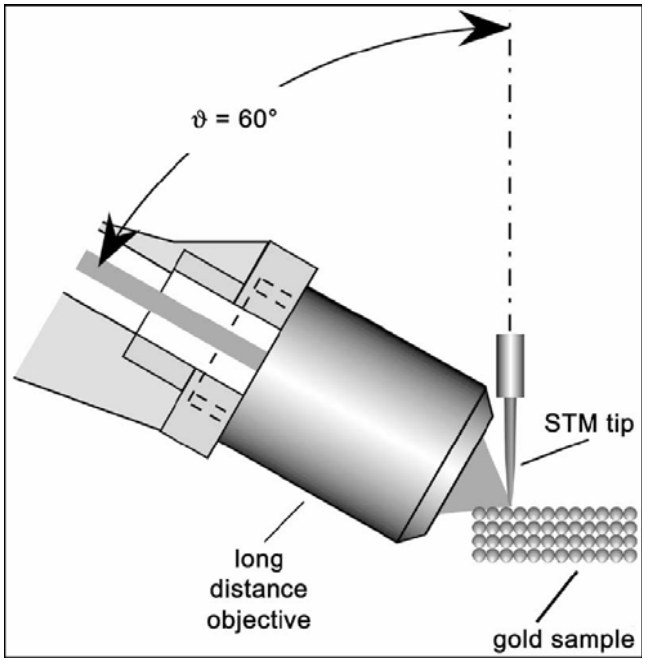

Enhanced Raman spectroscopy

Tip-enhanced enhanced Raman spectroscopy:

combining scanning tunneling microscopy and Raman spectroscopy.
enhancement due to gap modes.
flat surfaces can be investigated.

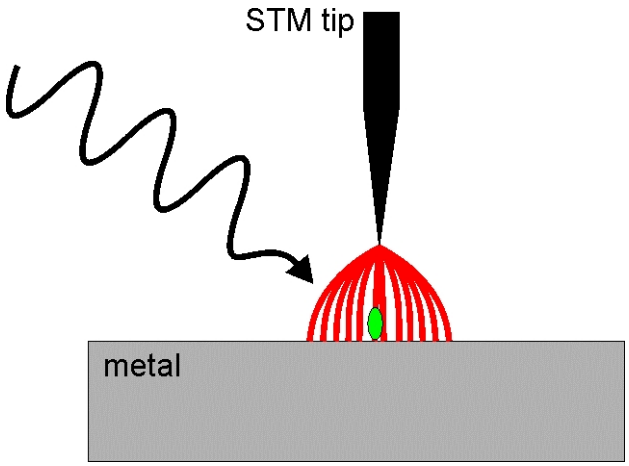

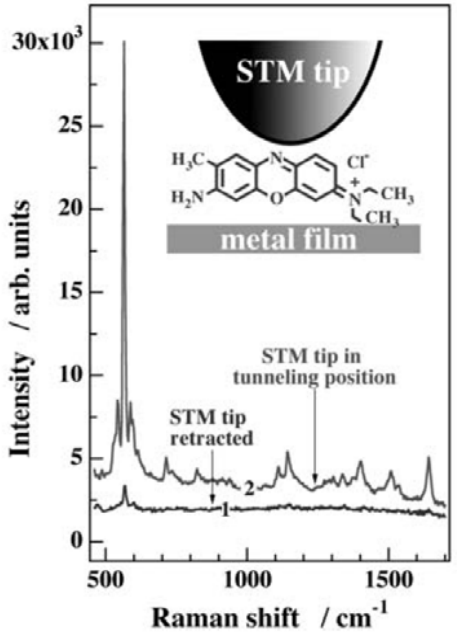

B. Pettinger et al., FHI

Surface vibrational sum frequency generation (SFG) spectroscopy

SFG is a second-order non-linear optical process that involves the mixing of tunable infrared light (ω_{IR}) with visible light of fixed frequency (ω_{VIS}) to produce a sum-frequency output ($\omega_{SFG} = \omega_{IR} + \omega_{VIS}$). In the electric dipole approximation, this process is allowed only in a medium without inversion symmetry, e.g. at surfaces.
The SFG process is resonantly enhanced if the energy of the infrared radiation matches a molecular vibration.
The intensity of the sum frequency signal depends on the absolute square of the second-order non-linear susceptibility and the intensities of the IR and VIS beams.

$$I_{SFG} \propto |\chi^{(2)}|^2 \bullet I_{IR} \bullet I_{VIS}$$

$\chi(2)$ contains a frequency-independent non-resonant contribution from the substrate und a resonant contribution of the molecule.

$$\chi_S^{(2)} = |\chi_{NR}^{(2)}| e^{i\varepsilon} + |\chi_R^{(2)}| e^{i\delta(\omega)}$$

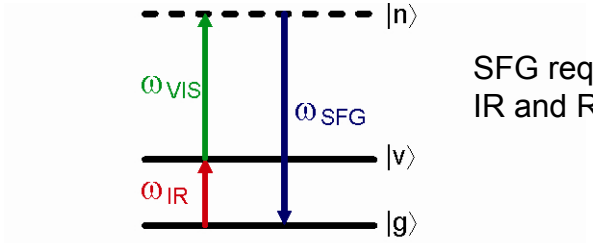

SFG requires
IR and Raman activity

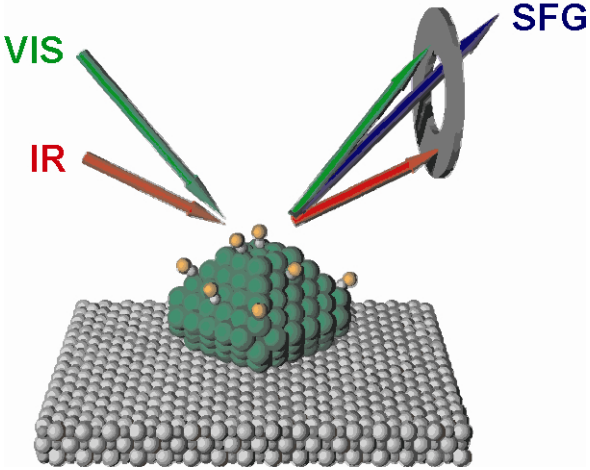

Surface vibrational sum frequency generation (SFG) spectroscopy

SFG in catalysis research:

high pressure experiments

no signal generated from the isotropic gas-phase

Experimental set-up

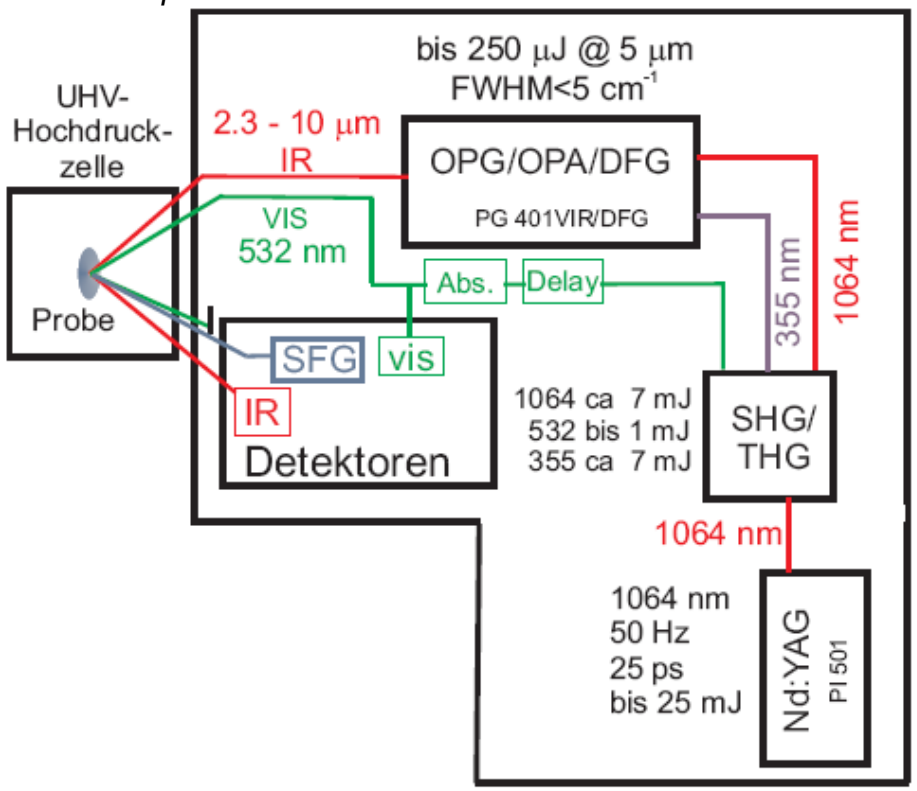

CO-Pd/Al_2O_3/NiAl(110)

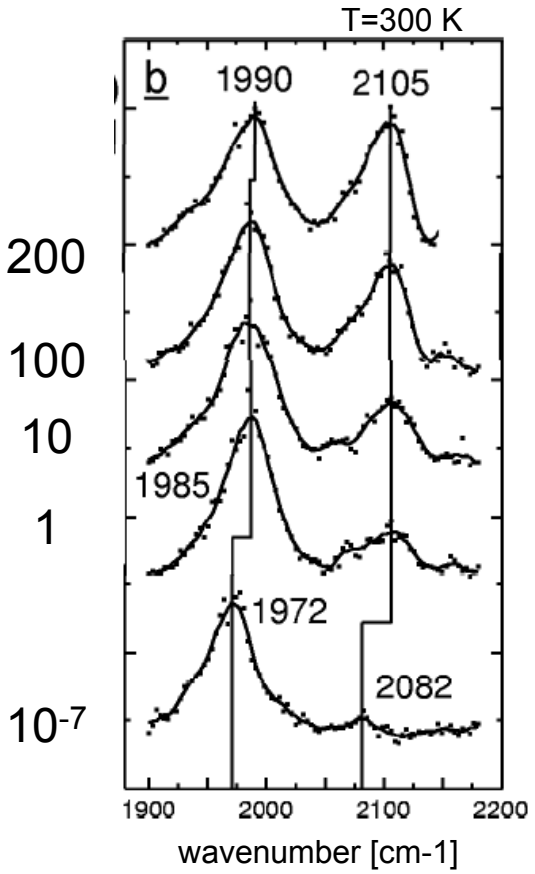

High resolution electron energy loss spectroscopy (HREELS)

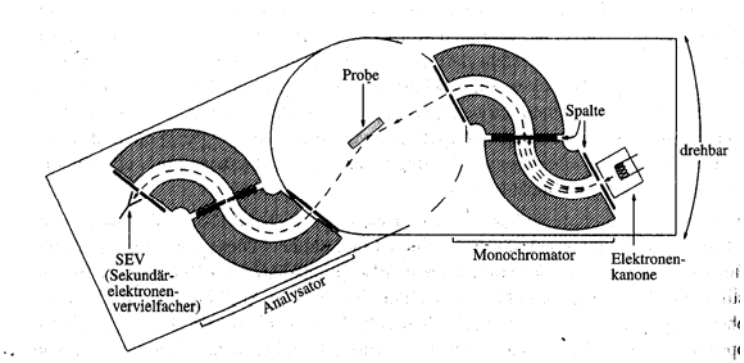

Bild 8.1: Elektronenenergieverlustspektrometer.

Inelastic scattering of low-energy electrons

Two scattering mechanisms:

Dipole scattering: incoming electron induces electric field perpendicular to the surface and excites only those vibrations that have a dipole moment normal to the surface.

Impact scattering: collision between electron and molecule, all vibrations excited; off-specular detection

Energy range: 50-5000 cm^{-1}

HREELS of $V_2O_5(001)$

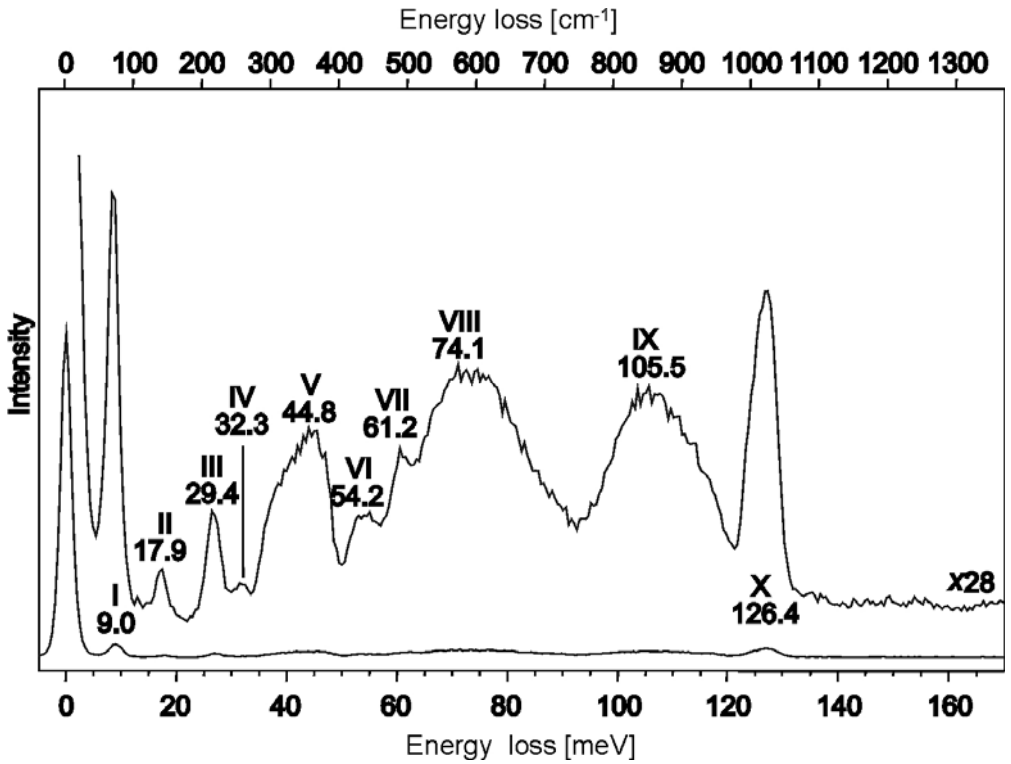

Inelastic electron tunneling spectroscopy – IETS

Metal – Insulator – Metal junction

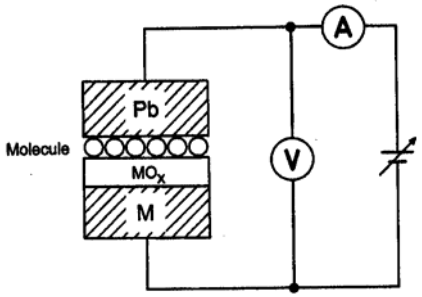

Fig. 1 Schematic representation of a tunneling junction. M, metal electrode; MO_x, metal oxide insulator; Pb, top lead electrode.

only for very thin (nm) insulating films
monolayer sensitivity
IR and Raman active modes

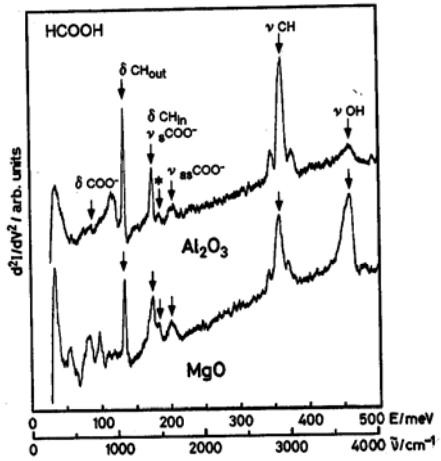

Fig. 7 Tunneling spectra of formic acid on Al_2O_3 and MgO doped from vapor.

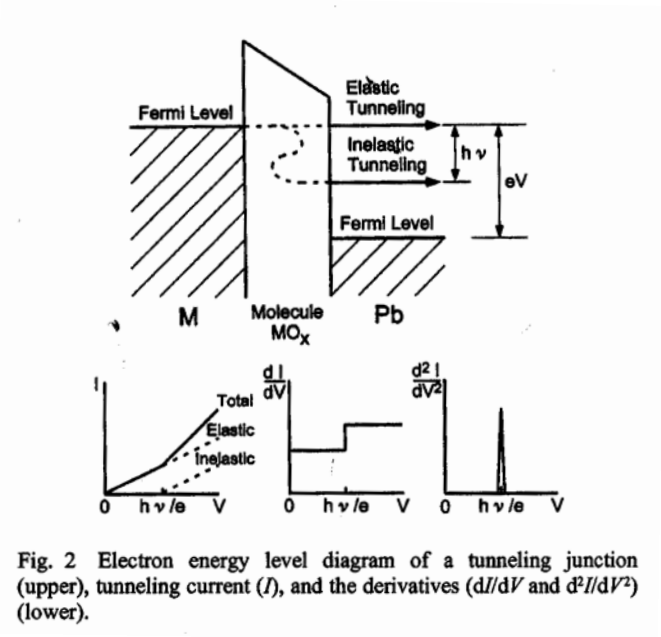

Fig. 2 Electron energy level diagram of a tunneling junction (upper), tunneling current (I), and the derivatives (dI/dV and d^2I/dV^2) (lower).

two kinds of tunneling currents:
-current due to elastic tunneling; steadily increasing from 0 V.
-current due to inelastic tunneling; threshold voltage ($h\nu/e$), corresponding to an molecular vibration.

kink in I-V curve
step in (dI/dV) curve
peak in (d^2I/dV^2) curve

Inelastic electron tunneling spectroscopy – IETS

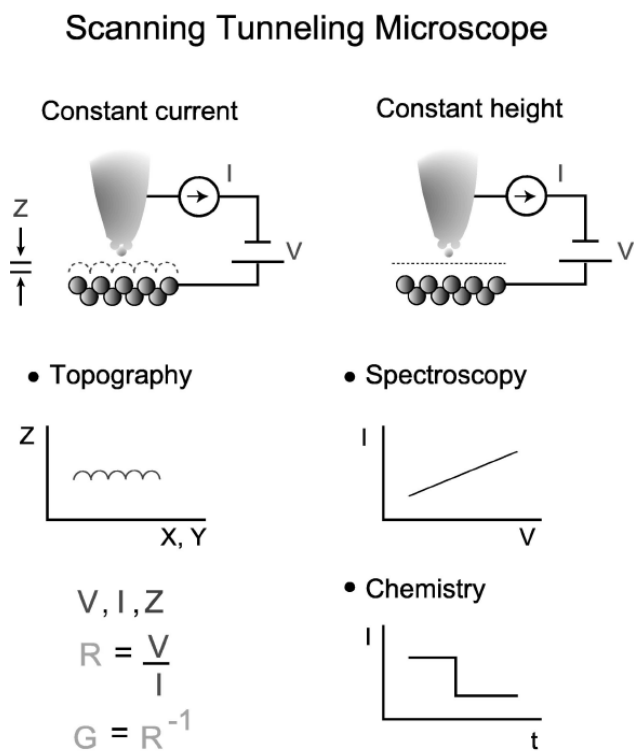

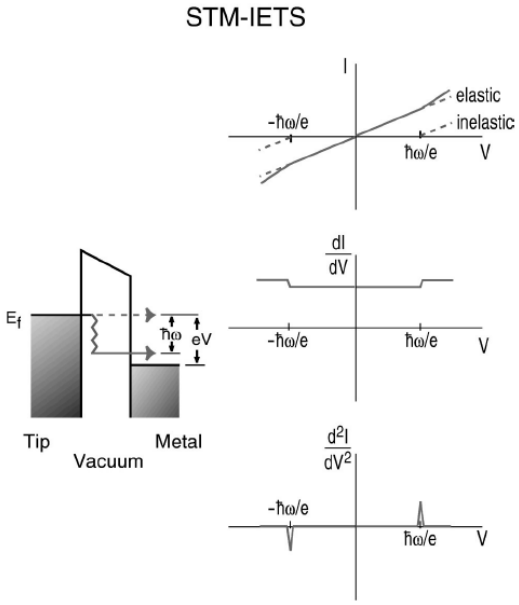

Different acetylene isotopes on Cu(001)

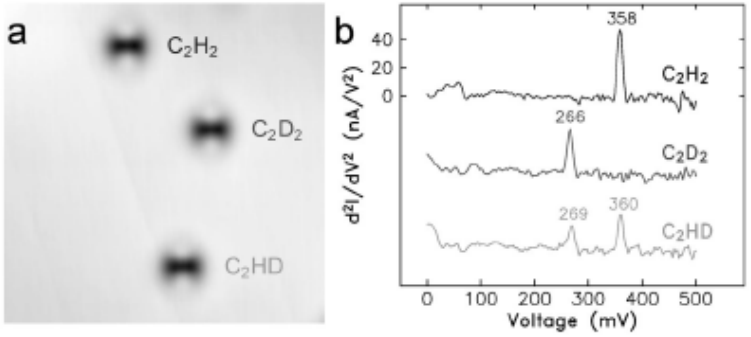

W. Ho et al.